Adaptive Flight Control in the Presence of Input Constraints

Amir F. Ajami

Thesis submitted to the Faculty of the
Virginia Polytechnic Institute and State University
in partial fulfillment of the requirements for the degree of

Master of Science
in
Aerospace Engineering

Dr. Naira Hovakimyan, Committee Chair
Dr. Hanspeter Schaub, Committee Member
Dr. Craig Woolsey, Committee Member

December 2, 2005
Blacksburg, Virginia

Keywords: Flight Control, Adaptive Control, Control Saturation

Adaptive Flight Control in the Presence of Input Constraints

Amir F. Ajami

(ABSTRACT)

Aerospace systems such as aircraft or missiles are subject to environmental and dynamical uncertainties. These uncertainties can alter the performance and stability of these systems. Adaptive control offers a useful means for controlling systems in the presence of uncertainties. However, very often adaptive controllers require more control effort than the actuator limits allow. In this thesis the original work of others on single input single output adaptive control in the presence of actuator amplitude limits is extended to multi-input systems. The Lyapunov based stability analysis is presented. Finally, the resultant technique is applied to aircraft and missile longitudinal motion. Simulation results show satisfactory tracking of the states of modified reference system.

Acknowledgments

This work would have not been completed without the help and support of many individuals. From those I like to name a few here.

First and for most I like to thank my advisor Dr. Hovakimyan for her passionate advices and support she gave me. She spent hours and days teaching me the principles of adaptive control. Even when I was away she used all means possible to educate me. Thank you Naira. Many thanks to Dr. Lavretsky from the Boeing company for his technical support and advices. I also would like to thank Vahram Stepanyan and Dr. Chengyu Cao for their help and patience while I worked with them.

I would also like to thank my committee members Dr. Hanspeter Schaub and Dr. Craig Woolsey for being there when I needed their advice and help. I thank the department of Aerospace and Ocean Engineering and Dr. Hovakimyan for supporting me through my education at Virginia Tech.

At last I like to thank my parents Nasrin and Ali for their unconditional love and support they gave me throughout my life. I wouldn't be here without them.

Contents

List of Figures

Chapter 1

Introduction

The X-15's beginnings were in 1952. It was the year of the first flight of the YB-52, and the aeronautical community was struggling to advance aircraft speeds from Mach 1.5 to Mach 2. Men of vision, however, already were looking to the higher speeds and altitudes that would eventually take us to orbital flight. For it was that year that the NACA Committee on Aeronautics recommended an increase in research dealing with flight to speeds of Mach 10 or 12 and to altitudes from 12 to 50 miles.

The X-15 was 50 feet long and had a wingspan of 22 feet. It weighed 33,000 pounds at launch and 15,000 pounds empty. Its flight control surfaces were hydraulically actuated and included all-moveable elevators, upper and lower rudders, speed brakes on the aft end of the fixed portion of the vertical fins, and landing flaps on the trailing edge of the wing. There were no ailerons; roll control was achieved by differential deflection of the horizontal tail.

All three X-15's were delivered with simple rate-feedback damping in all axes. The number three X-15, however, was extensively damaged during a ground run before it ever flew; when it was rebuilt it was fitted with a self-adaptive flight control system which included command augmentation, self-adaptive damper gains, several autopilot modes, and blended aerodynamic and ballistic controls.

The next flight resulting in the heat damage occurred in October 1967. In November of that year X-15 No.3 launched on what was planned to be a routine research flight to evaluate a boost guidance system and to conduct several other follow-on-experiments. During the boost, the airplane experienced an electrical problem that affected the flight control system and inertial displays. At peak altitude, the X-15 began a yaw to the right, and it re-entered the atmosphere yawed crosswise to the flight path. It went into a spin and eventually broke up at 65,000 feet, killing the pilot Michael Adams. It was later found that the adaptive control system was to be blamed for this incident.

Since the crash of X-15 more attention has been paid to robustness of adaptive controllers. While the main cause of that crash was parameter drift, as found out later, it was apparent that adaptive control theory was not ready for another flight for the next 30 years. Among many key issues control saturation plays a central role.

1.1 Motivation

The motivation and significance of the much needed design methods for adaptive control in the presence of input constraints can be illustrated today by control of unmanned aircraft, whose nominal flight control system is retrofitted with an adaptive element in order to track the guidance commands in the presence of failures and environmental uncertainties. If an unknown and/or undetected failure occurs (caused by battle damage or a control surface malfunction), then in spite of the failure, the guidance system would continue issuing its commands that may no longer be achievable by the aircraft. As a consequence, the required control effort will quickly saturate the aircraft surfaces while striving to maintain the "healthy" vehicle tracking performance, and subsequently will de-stabilize the aircraft. This situation may quickly become flight critical due to the fact that most of today's high performance aircraft are open-loop unstable.

Therefore, it is important to develop practical techniques to maintain stability of adaptive controllers in the presence of actuator amplitude saturation, or even avoid saturation to keep the vehicle on safer side. Today's airplanes utilize many actuators to control different surfaces. Thus there is a need to develop techniques that can be used for such multi-input flight systems.

1.2 Problem Definition

Consider the following system:

$$\dot{x}(t) = Ax(t) + B\Lambda u(t) \tag{1.1}$$

where $A \in \mathbb{R}^{n \times n}$ is the unknown system matrix, $B \in \mathbb{R}^{n \times m}$ is the known control power efficiency matrix, $\Lambda \in \mathbb{R}^{m \times m}$ is an unknown diagonal matrix with positive diagonal elements, usually introduced to model partial control surface failures, and $u \in \mathbb{R}^m$ is the control vector signal with amplitude saturation defined for each competent as follow:

$$u_i(t) \quad = \quad u_{\max_i} \operatorname{sat}\left(\frac{u_{c_i}(t)}{u_{\max_i}}\right) = \begin{cases} u_{c_i}(t), & |u_{c_i}(t)| \leq u_{\max_i} \\ u_{\max_i} \operatorname{sgn}\left(u_{c_i}(t)\right), & |u_{c_i}(t)| > u_{\max_i} \end{cases} \qquad i = 1, ..., m \tag{1.2}$$

In this thesis, we develop a method to ensure stable adaptation in the presence of input constraints (1.2).

1.3 Approach

The goal of this research is to use maximum possible control authority of an adaptive controller while maintaining satisfactory stability and tracking. The novel design approach is termed "Positive μ-modification", or simply "μ-mod", where the free design parameter μ defines a convex combination of the classical linear in parameters model reference adaptive control and a modified saturation bound. With this parameterization, the control deficiency can be reduced to ensure that the control signal *will never* incur saturation if needed. This reduction in control deficiency is achieved through a modification of the system command and its second derivative. This in turn may become crucial for preventing structural mode interaction problems during the periods of control saturation. Finally, Lyapunov based stability proofs are provided that define sufficient conditions on system parameters and reference input.

1.4 Overview

This thesis consists of four chapters. In chapter 2 we review previous results that have been derived in the area of adaptive control of aerospace systems in the presence of input constraints. In chapter 3 we first give the formulation of single input positive μ-mod modification applied to short period dynamics of aircraft and missiles. Next, we extend the single input positive μ-mod modification method to multi-input systems and show Lyapunov based stability proofs. In chapter 4 we apply the single-input and multi-input techniques to aircraft and missile longitudinal dynamics and show simulations. The thesis ends with chapter 5 that provides some recommendations for future work.

Chapter 2

Literature Review

2.1 Theory and Applications

In the past decade control design in the presence of input saturation has attracted a vast amount of research effort (for chronological bibliography see [4]). This issue is especially challenging in adaptive systems, because continued adaptation during input saturation may easily lead to instability. In order to overcome the undesirable/destabilizing effects of control saturation during the adaptation process, an adaptive modification (proportional to control deficiency) to both the tracking error and the reference model dynamics was proposed by Monopoli in [19] but without any formal proof of stability. In the Pseudo Control Hedging (PCH) method of Johnson and Calise [11] a fixed gain adjustment (proportional to control deficiency) to the reference model was introduced again without stability proofs. Authors in [21] show the formulation of discrete adaptive control with input saturation but without any Lyapunov based proofs. Ref. [1] provides stability proofs only when the parameter estimates converge before error converges. Ref.[22] also formulates techniques of modifying the reference states while providing no rigorous proofs. The author in [28] shows stability proofs of only stable adaptive controllers in the presence of input saturation. Refs. [18, 9] consider both amplitude and rate saturation for nonlinear systems without explicit construction of the domain of attraction.

Ref.[2] and Ref.[10] provide stability proofs of Model Reference Adaptive Control (MRAC) only for stable plants. Some earlier methods suggested stopping the adaptation during the saturation periods and reverting back to the nominal controller. Ref. [5] proposed adaptive scaling of the reference command (issued by guidance system) for preventing instabilities and failures of this type [12]. While all the previous works have focused on single input systems, Schawger in [25] extended the work of [12] to multi-input systems. In this work the author has tried to maintain the direction of control vector such that it remains within an ellipse inside the saturation limits. This method however does not allow the controller to use its maximum possible authority. Figure 2.1 shows the proposed control saturation function sat(u) used in [25] for stability proof.

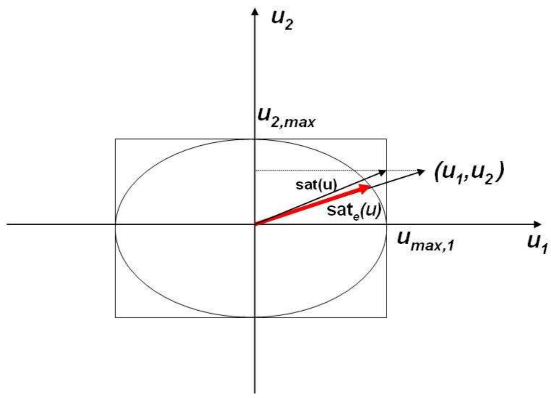

Figure 2.1: Elliptical saturation function.

From Figure 2.1 it can be seen that the saturation is defined such that the maximum control authority is the limit of the ellipse. In this case the direction of the control vector remains the same. This is done for the purpose of simplification of the stability proof. In this thesis we will develop the stability proof for the true saturation function sat(u) in Figure 2.1.

Chapter 3

Positive μ-Modification for Single Input Systems

This chapter is organized as follows. At first we state the problem formulation, then we present the control design approach by augmenting a baseline LQR controller with adaptive element, upon which we discuss the specifics of the μ-mod based design.

3.1 Problem Statement for Short Period Dynamics

An aircraft/missile short period dynamics can be written as:

$$\begin{bmatrix} \dot{\alpha}(t) \\ \dot{q}(t) \end{bmatrix} = \underbrace{\begin{bmatrix} Z_\alpha & 1 \\ M_\alpha & M_q \end{bmatrix}}_{A} \underbrace{\begin{bmatrix} \alpha(t) \\ q(t) \end{bmatrix}}_{\boldsymbol{x}(t)} + \lambda \underbrace{\begin{bmatrix} Z_\delta \\ M_\delta \end{bmatrix}}_{\boldsymbol{b}} (\delta(t) + f(\alpha(t), q(t))) \tag{3.1}$$

$$y(t) = \boldsymbol{c}^\top \boldsymbol{x}(t)\,, \tag{3.2}$$

where α is the angle of attack, q is the pitch rate, δ is the control surface (such as an elevator), M_α, M_q are the vehicle stability derivatives (partially known), while M_δ and Z_δ are the known/nominal values for control derivatives, λ is an unknown constant of known sign introduced to model control surface failure, $\boldsymbol{c}$ is a known vector, and $f(\alpha, q)$ denotes the uncertainty in the pitching moment.

In this section, we will address two different control objectives. For an F-16 model, we will set $\boldsymbol{c} = [0\ 1]^\top$ and design a full state feedback pitch rate tracking control $\delta_c(t)$. We will formulate reference model dynamics such that $q(t)$ tracks a commanded signal $r^{\text{cmd}}(t)$ in the presence of a static actuator model:

$$\begin{aligned}\delta(t) &= \delta_{\max}\,\text{sat}\left(\frac{\delta_c(t)}{\delta_{\max}}\right)\\ &= \begin{cases}\delta_c(t), & |\delta_c(t)| \le \delta_{\max}\\ \delta_{\max}\,\text{sgn}\left(\delta_c(t)\right), & |\delta_c(t)| > \delta_{\max}\end{cases}\quad.\end{aligned} \tag{3.3}$$

For a missile, we will perform an angle of attack tracking design while choosing $\boldsymbol{c} = [1\ 0]^\top$. The resultant simulations are shown in chapter 5.

3.2 Ideal Reference Model

For the short period dynamics above, in the absence of uncertainties and actuator constraints, the desired closed-loop reference model dynamics are derived using conventional LQR theory:

$$\begin{aligned}\begin{bmatrix}\dot{\alpha}_m^*(t)\\ \dot{q}_m^*(t)\end{bmatrix} &= A_m\underbrace{\begin{bmatrix}\alpha_m^*(t)\\ q_m^*(t)\end{bmatrix}}_{\boldsymbol{x}_m^*(t)} + \boldsymbol{b}k_g r^{\text{cmd}}(t)\\ y_m^*(t) &= \boldsymbol{c}^\top\boldsymbol{x}_m^*(t)\,,\end{aligned} \tag{3.4}$$

where

$$A_m = A_{\text{nom}} + \boldsymbol{b}\underbrace{\begin{bmatrix}k_{lqr_\alpha} & k_{lqr_q}\end{bmatrix}}_{\boldsymbol{k}_{lqr}^\top}, \tag{3.5}$$

in which A_{nom} is the matrix of the nominal (known) values of the stability derivatives, the gain $\boldsymbol{k}_{lqr}^\top = -r^{-1}\boldsymbol{b}^\top P$ is derived using the unique positive definite symmetric solution $P = P^\top > 0$ of the corresponding Riccati equation

$$Q + PA + A^\top P - P\boldsymbol{b}r^{-1}\boldsymbol{b}^\top P = 0$$

with $Q > 0$ being a positive definite symmetric weighting matrix, and r being the scalar control weight. The feedforward gain k_g is chosen to achieve a unity DC gain between the commanded signal $r(t)$ and the controlled system output $y(t)$.

$$k_g = -\frac{1}{\boldsymbol{c}^\top A_m^{-1}\boldsymbol{b}}\,. \tag{3.6}$$

3.3 Adaptive Control Design in the Absence of Control Saturation

For the system in (3.1), in the absence of control saturation an adaptive controller can be determined to track the reference model in (3.4) with bounded errors. In the presence control saturation, we need the following assumption to ensure the feasibility of the control objective.

Assumption 1 *There exists $R > 0$ such that $\forall \boldsymbol{x} \in \mathcal{B}_R \triangleq \{\boldsymbol{x} \in \mathbb{R}^2 : \|\boldsymbol{x}\| \le R\}$:*

$$\delta_{\max} \ge d \triangleq \max_{\boldsymbol{x}\in\mathcal{B}_R} |f(\boldsymbol{x})| \,. \tag{3.7}$$

Following [24], for all $\boldsymbol{x} \in \mathcal{B}_R \subset \mathbb{R}^2$, $\mathcal{B}_R \triangleq \{\boldsymbol{x} : \|\boldsymbol{x}\| \le R\}$ consider a parametrization of the unknown continuous nonlinearity $f(\alpha, q)$ using a linear combination of radial basis functions (RBFs) $\phi_i(\alpha, q)$:

$$f(\alpha, q) = \boldsymbol{\theta}^\top \boldsymbol{\Phi}(\alpha, q) + \varepsilon(\alpha, q), \quad |\varepsilon(\alpha, q)| \le \varepsilon^* \,, \tag{3.8}$$

where $\boldsymbol{\theta}$ is a vector of unknown constant coefficients $||\boldsymbol{\theta}|| \le \theta^*$, $\boldsymbol{\Phi}(\alpha, q)$ is a vector of Gaussian basis functions $\phi_i(\alpha, q)$, $|\phi_i(\alpha, q)| \le 1$, $\varepsilon(\alpha, q)$ represents the uniformly bounded approximation error, and ε^*, θ^* are known constants. Such approximation represents a linear in parameters neural network (NN) with RBFs in its inner layer. In the absence of control saturation, the model following adaptive controller is defined as:

$$\delta_{ad}(t) = \hat{\boldsymbol{k}}^\top(t)\boldsymbol{x}(t) + \hat{k}_r(t)r^{\text{cmd}}(t) - \hat{\boldsymbol{\theta}}^\top(t)\boldsymbol{\Phi}(\alpha(t), q(t)), \tag{3.9}$$

where $\hat{\boldsymbol{k}}(t)$, $\hat{k}_r(t)$, and $\hat{\boldsymbol{\theta}}(t)$ are the adaptive parameters. Following classical model reference adaptive control (MRAC) framework, we introduce the following matching assumptions:

$$\exists \boldsymbol{k}^* : \qquad A_m = A + \lambda \boldsymbol{b}(\boldsymbol{k}^*)^\top \tag{3.10}$$

$$\exists k_r^* : \qquad k_g = \lambda k_r^* \,. \tag{3.11}$$

Denoting $\tilde{\boldsymbol{k}}(t) = \hat{\boldsymbol{k}}(t) - \boldsymbol{k}^*$, $\tilde{k}_r(t) = \hat{k}_r(t) - k_r^*$, and $\tilde{\boldsymbol{\theta}}(t) = \hat{\boldsymbol{\theta}}(t) - \boldsymbol{\theta}$, the system dynamics in (3.1) with the control action (3.9) can be presented as:

$$\begin{aligned}\dot{\boldsymbol{x}}(t) &= A_m\boldsymbol{x}(t) + \lambda\boldsymbol{b}\hat{k}_r(t)r^{\text{cmd}}(t) + \lambda\boldsymbol{b}\tilde{\boldsymbol{k}}^\top(t)\boldsymbol{x}(t) - \lambda\boldsymbol{b}\tilde{\boldsymbol{\theta}}^\top(t)\boldsymbol{\Phi}(\alpha(t), q(t)) \\ &+ \lambda\boldsymbol{b}\varepsilon(\alpha(t), q(t)) \,.\end{aligned} \tag{3.12}$$

Subtracting (3.4) from (3.12), we obtain closed-loop error dynamics in the following form:

$$\begin{aligned}\dot{\boldsymbol{e}}(t) &= A_m\boldsymbol{e}(t) + \lambda\boldsymbol{b}\tilde{\boldsymbol{k}}^\top(t)\boldsymbol{x}(t) + \lambda\boldsymbol{b}\tilde{k}_r(t)r^{\mathrm{cmd}}(t) - \lambda\boldsymbol{b}\tilde{\boldsymbol{\theta}}^\top(t)\boldsymbol{\Phi}(\alpha(t),q(t))\\ &+\lambda\boldsymbol{b}\varepsilon(\alpha(t),q(t))\,,\end{aligned} \tag{3.13}$$

where

$$\boldsymbol{e}^\top(t) = [\alpha(t)-\alpha_m(t) \quad q(t)-q_m(t)] \tag{3.14}$$

is the tracking error. Consider the following adaptive laws:

$$\begin{aligned}\dot{\hat{\boldsymbol{k}}}(t) &= -\Gamma_{\boldsymbol{x}}\mathrm{Proj}(\hat{\boldsymbol{k}}(t), \boldsymbol{x}(t)\boldsymbol{e}^\top(t)P_0\boldsymbol{b}\mathrm{sgn}(\lambda))\\ \dot{\hat{k}}_r(t) &= -\gamma_r\mathrm{Proj}(\hat{k}_r(t), r^{\mathrm{cmd}}(t)\boldsymbol{e}^\top(t)P_0\boldsymbol{b}\mathrm{sgn}(\lambda))\\ \dot{\hat{\boldsymbol{\theta}}}(t) &= \Gamma_{\boldsymbol{\theta}}\mathrm{Proj}(\hat{\boldsymbol{\theta}}(t), \boldsymbol{\Phi}(\alpha(t),q(t))\boldsymbol{e}^\top(t)P_0\boldsymbol{b}\mathrm{sgn}(\lambda))\,,\end{aligned} \tag{3.15}$$

with the following initial conditions $\hat{\boldsymbol{k}}(0) = \boldsymbol{k}_{lqr}$, $k_r(0) = k_g$, $\hat{\boldsymbol{\theta}}(0) = 0$. In (3.15), $P_0 = P_0^\top > 0$ is the solution of the Lyapunov equation $A_m^\top P_0 + P_0A_m = -Q_0$ for some positive definite $Q_0 > 0$, $\mathrm{Proj}(\cdot,\cdot)$ denotes the projection operator [23] and ensures boundedness of adaptive parameters by definition, while $\Gamma_{\boldsymbol{x}}$, γ_r and $\Gamma_{\boldsymbol{\theta}}$ are the rates of adaptation. The derivative of the following candidate Lyapunov function

$$\begin{aligned}V(\boldsymbol{e}(t),\tilde{\boldsymbol{k}}(t),\tilde{k}_r(t),\tilde{\boldsymbol{\theta}}(t)) &= \boldsymbol{e}^\top(t)P_0\boldsymbol{e}(t) + |\lambda|\Big(\tilde{\boldsymbol{k}}^\top(t)\Gamma_{\boldsymbol{x}}^{-1}\tilde{\boldsymbol{k}}(t) + \tilde{k}_r^2(t)\gamma_r^{-1}\\ &+ \tilde{\boldsymbol{\theta}}^\top(t)\Gamma_{\boldsymbol{\theta}}^{-1}\tilde{\boldsymbol{\theta}}(t)\Big)\end{aligned} \tag{3.16}$$

along the trajectories of (3.13), (3.15) is

$$\dot{V}(t) = -\boldsymbol{e}^\top(t)Q_0\boldsymbol{e}(t) + \boldsymbol{e}^\top(t)P_0\boldsymbol{b}\varepsilon(\alpha(t),q(t))\,.$$

Therefore

$$\dot{V}(t) \le 0$$

if

$$||\boldsymbol{e}|| \ge \frac{2|\lambda| \;\; ||P_0\boldsymbol{b}||\varepsilon^*}{\lambda_{\min}(Q_0)},$$

where $\lambda_{\min}(Q_0)$ denotes the minimum eigenvalue of Q_0. Since the Projection operator ensures boundedness of parameter errors, then $\dot{V}(t) \le 0$ outside a compact set

$$\Big\{\|e\| \le \frac{2|\lambda| \; \|P_0\boldsymbol{b}\|\varepsilon^*}{\lambda_{\min}(Q_0)}\Big\}\bigcap\Big\{\|\tilde{W}\| \le W^*\Big\}, \tag{3.17}$$

where

$$\tilde{W}(t) = \Big[\tilde{\boldsymbol{k}}^\top(t) \;\; \tilde{k}_r(t) \;\; \tilde{\boldsymbol{\theta}}(t)\Big]$$

and W^* is the maximum allowable norm upper bound selected for the Projection operator, $\|\cdot\|$ denotes the 2-norm. Following standard invariant set arguments one can conclude that if the initial errors are within the largest level set of the Lyapunov function (3.16), for which the RBF approximation has been defined in (3.8), then the error dynamics (3.13) are ultimately bounded with respect to $\boldsymbol{e}(t)$, $\tilde{W}(t)$ and the ultimate bound is any number larger than the value of Lyapunov function on the minimum level set embracing the compact set in (3.17).

3.4 Positive μ-modification for Actuator Position Limits

The adaptive controller in (3.9) is not guaranteed to stay within the limits in (3.3), which may easily lead to instability. To overcome this, we introduce an adaptive modification of the reference model and modify the adaptive laws accordingly. Following the methodology in [16], we first define the pseudo-bound for the actuator position limit $\delta^*_{\max}$ as:

$$\delta^*_{\max} = 0.8\delta_{\max} \tag{3.18}$$

which means the safety zone is 20 % of saturation limit. Write the system dynamics in (3.1) as follows:

$$\dot{\boldsymbol{x}}(t) \quad = \quad A\boldsymbol{x}(t) + \lambda\boldsymbol{b}\left(\delta_c(t) + f(\alpha(t), q(t))\right) + \lambda\boldsymbol{b}\Delta\delta(t)\,, \tag{3.19}$$

where $\Delta\delta(t) = \delta(t) - \delta_c(t)$ denotes the control deficiency due to the static actuator model (3.3), and $\delta_c(t)$ is the commanded control signal. Consider the following μ-modification of the adaptive control signal:

$$\delta_c(t) \quad = \quad \delta_{ad}(t) + \mu\Delta\delta_c(t)\,, \tag{3.20}$$

where

$$\Delta\delta_c(t) = \delta^*_{\max}\ \mathrm{sat}\left(\frac{\delta_c(t)}{\delta^*_{\max}}\right) - \delta_c(t)$$

denotes the control deficiency due to the static actuator model in (3.3) with the pseudo-bound in (3.18), while $\mu > 0$ is a constant. In [16], it was shown that the implicit relationship in (3.20) has a unique explicit solution for the commanded control signal, which can be written as a convex combination of the adaptive control in the absence of control saturation defined in (3.9) and the pseudo-bound for the position limit in (3.18):

$$\begin{aligned}\delta_c(t) &= \frac{1}{1+\mu}\left(\delta_{ad}(t) + \mu\delta^*_{\max}\ \mathrm{sat}\left(\frac{\delta_{ad}(t)}{\delta^*_{\max}}\right)\right) \\ &= \begin{cases}\delta_{ad}(t), & |\delta_{ad}(t)| \le \delta^*_{\max} \\ \frac{1}{1+\mu}\left(\delta_{ad}(t) + \mu\delta^*_{\max}\right), & \delta_{ad}(t) > \delta^*_{\max} \\ \frac{1}{1+\mu}\left(\delta_{ad}(t) - \mu\delta^*_{\max}\right), & \delta_{ad}(t) < -\delta^*_{\max}\,. \end{cases}\end{aligned} \tag{3.21}$$

We note that setting $\mu = 0$ one recovers the adaptive control architecture from [12]. Substituting (3.20) into (3.19), we get:

$$\begin{aligned}\dot{\boldsymbol{x}}(t) &= A_m\boldsymbol{x}(t) - \lambda\boldsymbol{b}\tilde{\boldsymbol{k}}^\top(t)\boldsymbol{x}(t) - \lambda\boldsymbol{b}\tilde{\boldsymbol{\theta}}^\top(t)\boldsymbol{\Phi}(\alpha(t),q(t)) + \lambda\boldsymbol{b}\varepsilon(\alpha(t),q(t)) \\ &+ \lambda\boldsymbol{b}\Delta\delta_{ad}(t) - \boldsymbol{b}\lambda\hat{k}_r(t)r^{\mathrm{cmd}}(t)\,,\end{aligned} \tag{3.22}$$

where

$$\Delta\delta_{ad}(t) = \delta(t) - \delta_{ad}(t)\,.$$

This leads to the following modification of the adaptive reference model:

$$\begin{bmatrix}\dot{\alpha}_m(t) \\ \dot{q}_m(t)\end{bmatrix} = A_m \underbrace{\begin{bmatrix}\alpha_m(t) \\ q_m(t)\end{bmatrix}}_{\boldsymbol{x}_m(t)} + \boldsymbol{b}k_g(r^{\mathrm{cmd}}(t) + \hat{k}_u(t)\Delta\delta_{ad}(t))\,, \tag{3.23}$$

where $\hat{k}_u(t)$ is yet another adaptive gain and propagates according to the following dynamics:

$$\dot{\hat{k}}_u(t) = \gamma_u \mathrm{Proj}(\hat{k}_u(t), \Delta\delta_{ad}(t)\boldsymbol{e}^\top(t)P_0\boldsymbol{b}k_g). \tag{3.24}$$

In the above the ideal value of $\hat{k}_u(t)$ is:

$$k^*_u = \frac{\lambda}{k_g}.$$

As a result, modified closed-loop error dynamics can be derived as follows:

$$\begin{aligned}\dot{\boldsymbol{e}}(t) &= \dot{\boldsymbol{x}}(t) - \dot{\boldsymbol{x}}_m(t) \\ &= A_m\boldsymbol{e}(t) + \lambda\boldsymbol{b}\tilde{\boldsymbol{k}}^\top\boldsymbol{x}(t) - \lambda\boldsymbol{b}\tilde{\boldsymbol{\theta}}^T\boldsymbol{\Phi}(\alpha(t),q(t)) + \lambda\boldsymbol{b}\tilde{k}_r(t)r^{\mathrm{cmd}}(t) + \lambda\boldsymbol{b}\varepsilon(\alpha(t),q(t)) \\ &- \boldsymbol{b}k_g\tilde{k}_u(t)\Delta\delta_{ad}(t)\,,\end{aligned} \tag{3.25}$$

where $\tilde{k}_u(t) = \hat{k}_u(t) - k^*_u$. Define the following candidate Lyapunov function:

$$\begin{aligned}V(\boldsymbol{e}(t),\tilde{\boldsymbol{k}}(t),\tilde{k}_r(t),\tilde{k}_u(t),\tilde{\boldsymbol{\theta}}(t)) &= \boldsymbol{e}^\top(t)P_0\boldsymbol{e}(t) + |\lambda|(\tilde{\boldsymbol{k}}^\top(t)\Gamma^{-1}_{\boldsymbol{x}}\tilde{\boldsymbol{k}}(t) + \tilde{k}^2_r(t)\gamma_r \\ &+ \tilde{\boldsymbol{\theta}}^\top(t)\Gamma^{-1}_{\boldsymbol{\theta}}\tilde{\boldsymbol{\theta}}(t)) + \gamma^{-1}_u\tilde{k}^2_u(t)\end{aligned} \tag{3.26}$$

Its time derivative along the trajectories of (3.25) along with the adaptive laws in (3.15) and (3.24) is:

$$\begin{aligned}\dot{V}(\boldsymbol{e}(t), \tilde{\boldsymbol{k}}(t), \tilde{k}_r(t), \tilde{k}_u(t), \tilde{\boldsymbol{\theta}}(t)) &= -\boldsymbol{e}^\top(t) Q_0 \boldsymbol{e}(t) + 2\lambda \boldsymbol{e}^\top(t) P_0 \boldsymbol{b} \varepsilon(\alpha(t), q(t)) \\ &\leq -\lambda_{\min}(Q_0)||\boldsymbol{e}(t)||^2 + 2\lambda||\boldsymbol{e}(t)||||P_0\boldsymbol{b}||\varepsilon^* \\ &\leq -||\boldsymbol{e}(t)||[\lambda_{\min}(Q_0)||\boldsymbol{e}(t)|| - 2||P_0\boldsymbol{b}||\varepsilon^*] \qquad (3.27)\end{aligned}$$

Hence

$$\dot{V}(t) \leq 0$$

if

$$||\boldsymbol{e}|| \geq \frac{2||P_0\boldsymbol{b}||\varepsilon^*}{\lambda_{\min}(Q_0)}.$$

To prove that the solutions of (3.15), (3.24) and (3.25) are Lyapunov bounded, one needs to prove additionally that the adaptive reference model in (3.23) stays bounded with the given modification. In [16], in the absence of nonlinearity, a constructive proof is developed and a domain of attraction for the μ-modification based adaptive control is derived explicitly. It is shown in [16] that for open-loop stable systems the method leads to globally stable asymptotic tracking of the modified reference model. For open-loop unstable systems the domain of attraction of system states is constructed explicitly, for which local asymptotic stability can be proved. In [17], the method is extended to systems with matched nonlinearities, and an RBF approximation is introduced to compensate for the effects of the latter. Due to the approximation nature of RBFs, the results are local both for open-loop stable and unstable systems. The main theorem from [17] can be summarized:

Theorem 1 *Let Assumption 1 hold with R satisfying*

$$R > \frac{2\lambda\,|\delta_{\max} - d|\,\|P\boldsymbol{b}\|}{\kappa} \qquad (3.28)$$

Further let A and $\boldsymbol{b}$ in (3.1), $\delta_{\max}$ in (3.3), $r_{\max} \triangleq \max_{t\in[0,\infty)} r^{\text{cmd}}(t)$ and $Q_0 > 0$ be such that

$$r_{\max} < \frac{\lambda_{\min}(Q_0)|\delta_{\max} - d| - \varepsilon^*\sqrt{\rho}\kappa}{|k_r^*|\sqrt{\rho}\kappa},$$

where $P_0 = P_0^\top > 0$ is the unique solution of the algebraic Lyapunov equation, while $\rho = \frac{\lambda_{\max}(P_0)}{\lambda_{\min}(P_0)}$, $\kappa = \left|\lambda_{\min}(Q_0) - 2\lambda\|P\boldsymbol{b}\|\|\boldsymbol{k}^*\|\right|$. If the system initial conditions and the initial value of the Lyapunov function in (4.41) satisfy:

$$\boldsymbol{x}^\top(0)P_0\boldsymbol{x}(0) < \lambda_{\min}(P_0)\left[\frac{2\lambda\|P_0\boldsymbol{b}\|}{\kappa}\,|u_{\max} - d|\right]^2$$

$$\sqrt{V(0)} < \sqrt{\frac{|\lambda|}{\lambda_{\max}(\Gamma_{\boldsymbol{x}})}} \frac{\lambda_{\min}(Q_0) - \sqrt{\rho}\ \frac{|k_r^*|\ r_{\max}+\varepsilon^*}{|\delta_{\max}-d|}\kappa}{2\lambda\|P_0\boldsymbol{b}\| + \sqrt{\rho}\ \frac{\beta_1 r_{\max}+\beta_2 N}{|u_{\max}-d|}\kappa}$$

where $\beta_1 \triangleq \frac{\tilde{k}^{\max}}{\tilde{k}_r^{\max}}$, $\beta_2 \triangleq \frac{\tilde{\theta}^{\max}}{\tilde{k}_r^{\max}}$, *and* $\|\tilde{\boldsymbol{k}}\| \leq \tilde{k}^{\max}$, $\|\tilde{k}_r\| \leq \tilde{k}_r^{\max}$, $\|\tilde{\boldsymbol{\theta}}\| \leq \tilde{\theta}^{\max}$ *are guaranteed via the projection operator, then the adaptive system with μ-modification has bounded solutions* $\forall r^{\text{cmd}}(t)$, $|r^{\text{cmd}}(t)| \leq r_{\max}$, *and* $\forall t > 0$

$$\boldsymbol{x}^\top(t)P_0\boldsymbol{x}(t) < \lambda_{\min}(P_0)\left[\frac{2\lambda\|P_0\boldsymbol{b}\|}{\kappa}\,|\delta_{\max} - d|\right]^2 .$$

Chapter 4

Adaptive Control for Multi-input Systems in the Presence of Control Constraints

4.1 Mathematical Preliminaries on Multi-Input Control Saturation

Consider an m dimensional vector $y \in \mathbb{R}^m$ and introduce the saturation function as follow:

$$\mathrm{sat}(y) = \begin{pmatrix} \mathrm{sat}(y_1) \\ \vdots \\ \mathrm{sat}(y_m) \end{pmatrix} \tag{4.1}$$

where $\mathrm{sat}(y_i)$ is defined as:

$$\mathrm{sat}(y_i) = \begin{cases} y_i, & |y_i| \leq 1 \\ \mathrm{sgn}(y_i), & |y_i| > 1 \end{cases} \tag{4.2}$$

Recall that the ∞-norm of a vector is:

$$\|y\|_\infty = \mathrm{max}_i |y_i|$$

Assuming that $y \neq 0$, scale the vector y by its ∞-norm and let

$$y_{\perp} = \frac{y}{\|y\|_{\infty}}$$

From simple geometrical considerations it follows that $y_{\perp}$ is the projection of y onto a unit cube, where the latter is understood in terms of the ∞-norm. The projection $y_{\perp}$ touches one of the sides of the unit cube $\|y\|_{\infty} \leq 1$, which, in turn, defines the saturation limits for each of the components of the vector y. Notice that $y_{\perp}$ is a direction preserving scaled version of the original vector y and it does not violate the saturation constraints (Figure 4.1). Also, from definitions in (4.1) and (4.2) we rewrite sat(y) as:

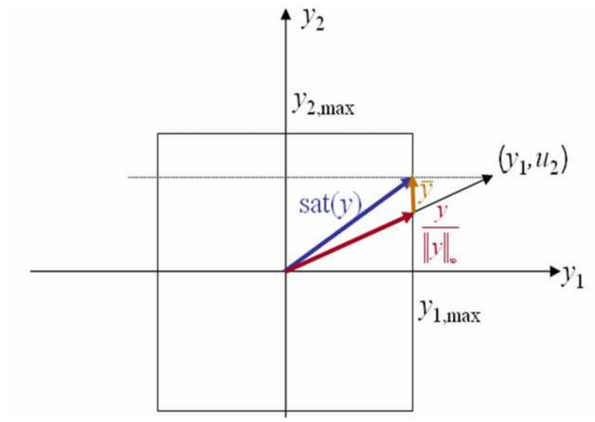

Figure 4.1: Saturation of two dimensional vector.

$$\text{sat}(y) = \begin{cases} y, & \|y\|_{\infty} \leq 1 \\ y_{\perp} + \overline{y}, & \|y\|_{\infty} > 1 \end{cases} \tag{4.3}$$

where the components of the newly introduced vector $\overline{y}$ are:

$$\overline{y}_i = \text{sat}(y_i) - y_{\perp_i} = \begin{cases} y_i - y_{\perp_i}, & |y_i| \leq 1 \\ \text{sgn}(y_i), & |y_i| > 1 \end{cases}$$

Notice that

$$\overline{y}_i = \begin{cases} (1 - \frac{1}{\|y\|_{\infty}})y_i, & |y_i| \leq 1 \\ \\ (1 - \|y_{\perp_i}\|_2)\text{sgn}(y_i), & |y_i| > 1 \end{cases} \tag{4.4}$$

Therefore

$$|\overline{y}_i| = \begin{cases} |\,1 - \frac{1}{\|y\|_\infty}||y_i|, & |y_i| \leq 1 \\ \\ |1 - \frac{|y_i|}{\|y\|_\infty}|, & |y_i| > 1 \end{cases} \tag{4.5}$$

The following upper bound is true:

$$|\overline{y}_i| \leq \left|1 - \frac{1}{\|y\|_\infty}\right|. \tag{4.6}$$

Therefore, if $\|y\|_\infty > 1$, from (4.6) it follows that $|\overline{y}_i| < 1$ for all $i = 1, 2, ..., m$. Hence, $\|\overline{y}\|_\infty < 1$ or

$$\|y\|_\infty > 1 \Rightarrow \|\overline{y}\|_\infty < 1 \Rightarrow \|\overline{y}\|_\infty < \|y\|_\infty \tag{4.7}$$

Figure (4.1) shows a two dimensional vector during the saturation.

Let $\|y\|_2 = \sqrt{y^\top y}$ be the *Euclidean* norm of y. Then

$$\|y\|_\infty \leq \|y\|_2 \leq \sqrt{m}\|y\|_\infty$$

or

$$\frac{\|y\|_2}{\sqrt{m}} \leq \|y\|_\infty \leq \|y\|_2 \tag{4.8}$$

Using (4.8) in (4.7) for $\|y\|_\infty > 1$, we have

$$\|\overline{y}\|_2 < \sqrt{m}\|\overline{y}\|_\infty < \sqrt{m}\|y\|_\infty < \sqrt{m}\|y\|_2 \tag{4.9}$$

Lemma 4.1 *For the Euclidean norms of the vectors y and $\overline{y}$, if $\|y\|_\infty > 1$, the following inequalities are true:*

$$0 < \|\mathrm{sat}(y)\|_2 - \|\overline{y}\|_2 \leq \sqrt{m} \tag{4.10}$$

Proof. Indeed,

$$|\|\mathrm{sat}(y)\|_2 - \|\overline{y}\|_2| \leq \|\mathrm{sat}(y) - \overline{y}\|_2 = \|y_\perp\|_2 = \frac{\|y\|_2}{\|y\|_\infty} \leq \frac{\sqrt{m}\|y\|_\infty}{\|y\|_\infty} = \sqrt{m}$$

On the other hand, to prove that $0 < \|\mathrm{sat}(y)\|_2 - \|\overline{y}\|_2$, it is sufficient to prove that

$$(\|\mathrm{sat}(y)\|_2 - \|\overline{y}\|)(\|\mathrm{sat}(y)\|_2 + \|\overline{y}\|_2) = \|\mathrm{sat}(y)\|_2^2 - \|\overline{y}\|_2^2 = \sum_{i=1}^{m}((\mathrm{sat}(y_i))^2 - (\overline{y}_i)^2) > 0 \tag{4.11}$$

To this end, notice that from (4.2) and (4.4) we conclude

$$(\mathrm{sat}(y_i))^2 - (\overline{y}_i)^2 = \begin{cases} y_i^2 - (1 - \frac{1}{\|y\|_\infty})^2 y_i^2, & |y_i| \le 1 \\ \\ 1 - (1 - \frac{|y_i|}{\|y\|_\infty})^2, & |y_i| > 1 \end{cases}$$

If $\|y\|_\infty > 1$, then

$$0 < \left(1 - \frac{1}{\|y\|_\infty}\right)^2 < 1$$

At the same time, from the definition of $\|y\|_\infty$ we get

$$0 \le \left(1 - \frac{|y_i|}{\|y\|_\infty}\right)^2 \le 1.$$

Since $\|y\|_\infty > 1$, then $y \neq 0$, and therefore there exists at least one i for which the following can be true:

$$0 \le \left(1 - \frac{|y_i|}{\|y\|_\infty}\right)^2 < 1$$

Hence

$$\sum_{i=1}^{m} ((\mathrm{sat}(y_i))^2 - (\overline{y}_i)^2) > 0$$

Thus the lower bound in (4.11) holds and,

$$\|\mathrm{sat}(y)\|_2 - \|\overline{y}\|_2 > 0,$$

which leads to (4.10). The proof is complete.

In case of arbitrary non-equal bounds, let

$$X_{\max} = \begin{bmatrix} X_{\max_1} & \dots & 0 \\ \vdots & \ddots & \vdots \\ 0 & \dots & X_{\max_m} \end{bmatrix}$$

and let

$$y = X_{\max}^{-1} x$$

Then, it can be seen that the projection of y onto a unit cube (defined by the ∞-norm) is equivalent to the projecting vector x onto m-dimensional rectangle with each side bounded by $X_{\max_i}$.

4.2 Problem Formulation

Let the system dynamics propagate according to the following differential equation:

$$\dot{\boldsymbol{x}}(t) = A\boldsymbol{x}(t) + B\Lambda\boldsymbol{u}(t) \tag{4.12}$$

where $\boldsymbol{x} \in \mathbb{R}^n$ is the state of the system, $\boldsymbol{u} \in \mathbb{R}^m$ is the control input, A is an unknown $(n \times n)$ matrix, B is a known $(n \times m)$ constant matrix, Λ is an unknown $(n \times n)$ constant diagonal matrix with positive diagonal elements. The control input $\boldsymbol{u} \in \mathbb{R}^m$ is amplitude limited and is calculated using the following static actuator model:

$$\boldsymbol{u}(t) = \begin{pmatrix} u_{\max_1}\mathrm{sat}(\frac{u_{c_1}(t)}{u_{\max_1}}) \\ \vdots \\ u_{\max_m}\mathrm{sat}(\frac{u_{c_m}(t)}{u_{\max_m}}) \end{pmatrix} \tag{4.13}$$

Here, $u_{c_1}(t), ..., u_{c_m}(t)$ are the components of the commanded vector of control input $\boldsymbol{u}_c(t)$, while $u_{\max_1}, ..., u_{\max_m}$ are the actuator saturation limits. Equivalently, we can rewrite (4.13) as:

$$\boldsymbol{u}(t) = U_{\max}\mathrm{sat}(U_{\max}^{-1}\boldsymbol{u}_c(t)) \tag{4.14}$$

where

$$U_{\max} = \begin{bmatrix} u_{\max_1} & \dots & 0 \\ \vdots & \ddots & \vdots \\ 0 & \dots & u_{\max_m} \end{bmatrix}$$

Thus for $i = 1, ..., m$ component-wise one obtains:

$$u_i(t) = u_{\max_i}\mathrm{sat}\left(\frac{u_{c_i}(t)}{u_{\max_i}}\right) = \begin{cases} u_{c_i}(t), & |u_{c_i}(t)| \le u_{\max_i} \\ \\ u_{\max_i}\mathrm{sgn}(u_{c_i}(t)), & |u_{c_i}(t)| > u_{\max_i} \end{cases} \tag{4.15}$$

Lemma 4.2 *For any $\boldsymbol{u}_c(t) \in \mathbb{R}^m$ there exists a bounded vector $\overline{\boldsymbol{u}}(t) \in \mathbb{R}^m$ such that $\forall t > 0$ the output of the static actuator model (4.14)-(4.15) can be written as:*

$$\boldsymbol{u}(t) = \begin{cases} \boldsymbol{u}_c(t), & \|U_{\max}^{-1}\boldsymbol{u}_c(t)\|_\infty \le 1 \\ \\ \boldsymbol{u}_{c_\perp}(t) + \overline{\boldsymbol{u}}(t), & \|U_{\max}^{-1}\boldsymbol{u}_c(t)\|_\infty > 1 \end{cases} \tag{4.16}$$

where $\boldsymbol{u}_{c_\perp}(t) = \frac{\boldsymbol{u}_c(t)}{\|U_{\max}^{-1}\boldsymbol{u}_c(t)\|_\infty}$, *and the components of* $\overline{\boldsymbol{u}}(t)$ *are*

$$\overline{u}_i(t) = \begin{cases} u_{c_i}(t) - u_{c_{\perp i}}(t), & |u_{c_i}(t)| \le u_{\max_i} \\ \\ \mathrm{sgn}(u_{c_i}(t)) - u_{c_{\perp i}}(t), & |u_{c_i}(t)| > u_{\max_i} \end{cases}$$

The proof follows from definitions in (4.14) and (4.15).

From Lemma 3.1 and the relationships in 4.9 it follows that

$$\|\overline{\boldsymbol{u}}(t)\| < \|\boldsymbol{u}(t)\| \le \sqrt{m}u_{\max}, \tag{4.17}$$

where $u_{\max} = \max\{u_{\max_1}, ..., u_{\max_m}\}$.

Rewriting system dynamics in (4.12) by adding and subtracting $\boldsymbol{u}_c(t)$ from $\boldsymbol{u}(t)$ we get:

$$\dot{\boldsymbol{x}}(t) = A\boldsymbol{x}(t) + B\Lambda\boldsymbol{u}_c(t) + B\Lambda\Delta\boldsymbol{u}(t) \tag{4.18}$$

where $\Delta\boldsymbol{u}(t) = \boldsymbol{u}(t) - \boldsymbol{u}_c(t)$ denotes the *control deficiency* due to the amplitude saturation limits of actuators:

$$\Delta\boldsymbol{u}(t) = [\Delta u_1(t), ..., \Delta u_m(t)]^\top, \tag{4.19}$$

$$\Delta u_i(t) = \begin{cases} 0, & |u_{c_i}(t)| \le u_{\max_i} \\ \\ (u_{\max_i} - |u_{c_i}|)\mathrm{sgn}(u_{c_i}(t)), & |u_{c_i}(t)| > u_{\max_i} \end{cases} \tag{4.20}$$

Notice that from (4.16) we can write

$$\Delta\boldsymbol{u}(t) = \begin{cases} 0, & \|U_{\max}^{-1}\boldsymbol{u}_c(t)\|_\infty \le 1 \\ \\ \boldsymbol{u}_{c_\perp}(t) + \overline{\boldsymbol{u}}(t) - \boldsymbol{u}_c(t), & \|U_{\max}^{-1}\boldsymbol{u}_c(t)\|_\infty > 1 \end{cases} \tag{4.21}$$

Consider the following reference model dynamics, driven by a uniformly bounded continuous reference input $\{\boldsymbol{r} \in \mathbb{R}^m : \|\boldsymbol{r}(t)\| \le r_{\max}\}$:

$$\dot{\boldsymbol{x}}_m^*(t) = A_m\boldsymbol{x}_m^*(t) + B_m\boldsymbol{r}(t) \tag{4.22}$$

In (4.22), $\boldsymbol{x}_m^*(t) \in \mathbb{R}^n$ is the state of the reference model, A_m^* is Hurwitz matrix, $B_m \in \mathbb{R}^{n\times m}$, and the pair (A_m, B_m) is controllable. The control design problem, addressed in this chapter, can be stated as follows:

Given reference model (4.22), define an adaptive control architecture $\boldsymbol{u}_c(t)$ and, if necessary, augment the input $\boldsymbol{r}(t)$ to the reference model, so that the state $\boldsymbol{x}(t)$ of the system (4.12) in the presence of multi-input constraints (4.14) tracks the state of $\boldsymbol{x}_m(t)$ of the augmented reference model asymptotically, while all the signals in both systems remain bounded.

4.3 Positive μ-modification and Closed Loop System Dynamics

The main challenge in designing an adaptive controller for the system in (4.12), (4.14) is associated with the control deficiency $\Delta \boldsymbol{u}(t) = \boldsymbol{u}(t) - \boldsymbol{u}_c(t)$ that appears in (4.18). Using this signal, in [25] a modification to the reference model dynamics was suggested and the corresponding direct adaptive laws were formulated. Motivated by [25], we propose yet another control design modification that protects the adaptive input signal from position saturation. To this end, choose constants $0 < \delta_i < u_{\max_i}$, where $i = 1, ..., m$, and define $u^{\delta_i}_{\max_i} = u_{\max_i} - \delta_i$ for every $i = 1, ..., m$. Then the control deficiency can be represented as:

$$\Delta \boldsymbol{u}(t) = \Delta \boldsymbol{u}_c(t) + \Delta_{\text{sat}}(t) \tag{4.23}$$

where

$$\Delta u_{c_i}(t) = u^{\delta_i}_{\max_i} \text{sat}\left(\frac{u_{c_i}(t)}{u^{\delta_i}_{\max_i}}\right) - u_{c_i}(t), \quad i = 1, ..., m \tag{4.24}$$

$$\Delta_{\text{sat}_i}(t) = u_{\max_i} \text{sat}\left(\frac{u_{c_i}(t)}{u_{\max_i}}\right) - u^{\delta_i}_{\max_i} \text{sat}\left(\frac{u_{c_i}(t)}{u_{\max_i}}\right), \quad i = 1, ..., m \tag{4.25}$$

Direct adaptive model reference control architecture with μ-modification is defined as:

$$\boldsymbol{u}_c(t) = \boldsymbol{u}_{ad}(t) + \mu \Delta \boldsymbol{u}_c(t), \tag{4.26}$$

$$\boldsymbol{u}_{ad}(t) = K_x^\top(t)\boldsymbol{x}(t) + K_r^\top(t)\boldsymbol{r}(t) \tag{4.27}$$

In (4.26), $\boldsymbol{u}_{ad}(t)$ denotes the conventional linear in parameters adaptive control, $K_x(t) \in \mathbb{R}^{n\times m}$, $K_r(t) \in \mathbb{R}^{m\times m}$ are adaptive gains, and $\mu \in \mathbb{R}^{m\times m}$ is a diagonal matrix of design constants $\mu_1, ..., \mu_m$. Note that the relation (4.26) defines the commanded control input $\boldsymbol{u}_c(t)$ implicitly. Next, we show that explicit solution of the latter can be found.

Lemma 4.3 If $\mu_1, ..., \mu_m \geq 0$, then the solution to (4.26) is given by a convex combination of $\boldsymbol{u}_{ad}(t)$ and $\boldsymbol{u}^{\delta}_{\max}\text{sat}\left(\frac{\boldsymbol{u}_{ad}(t)}{\boldsymbol{u}^{\delta}_{\max}}\right) \quad \forall t > 0:$

$$\boldsymbol{u}_c(t) = (I_m + \mu)^{-1}(\boldsymbol{u}_{ad}(t) + \mu\tilde{U}_{\max}\text{sat}(\tilde{U}^{-1}_{\max}\boldsymbol{u}_{ad}(t))) \tag{4.28}$$

which also can be represented component wise in the following form:

$$u_{c_i}(t) = \begin{cases} u_{ad_i}(t), & |u_{ad_i}(t)| \leq u^{\delta_i}_{\max_i} \\ \frac{1}{1+\mu_i}\left(u_{ad_i}(t) + \mu_i u^{\delta_i}_{\max_i}\right), & u_{ad_i}(t) > u^{\delta_i}_{\max_i} \\ \frac{1}{1+\mu_i}\left(u_{ad_i}(t) - \mu_i u^{\delta_i}_{\max_i}\right), & u_{ad_i}(t) < -u^{\delta_i}_{\max_i} \end{cases} \tag{4.29}$$

with $i = 1, ..., m$.

Proof. If $|u_{c_i}| \leq u^{\delta_i}_{\max_i}$, then $\Delta u_{c_i}(t) = 0$, and the first relationship in (4.29) takes place. If $|u_{c_i}(t)| > u^{\delta_i}_{\max_i}$, then using (4.24) along with (4.15) and (4.26), we can get:

$$u_{c_i}(t) = u_{ad_i}(t) + \mu_i \underbrace{\left(u^{\delta_i}_{\max_i}\text{sgn}(u_{c_i}(t)) - u_{c_i}(t)\right)}_{\Delta u_{c_i}(t)} \tag{4.30}$$

or equivalently

$$\begin{aligned} u_{c_i}(t) &= \frac{1}{1+\mu_i}\left(u_{ad_i}(t) + \mu_i u^{\delta_i}_{\max_i}\text{sgn}(u_{c_i}(t))\right) \\ &= \begin{cases} \frac{1}{1+\mu_i}\left(u_{ad_i}(t) + \mu_i u^{\delta_i}_{\max_i}\right), & u_{c_i} > u^{\delta}_{\max_i} \\ \frac{1}{1+\mu_i}\left(u_{ad_i}(t) - \mu_i u^{\delta_i}_{\max_i}\right), & u_{c_i} < -u^{\delta}_{\max_i} \end{cases} \end{aligned} \tag{4.31}$$

It can be seen that since $\mu_i \geq 0$, the second and the third lines in the above relationship are equivalent to the corresponding ones in (4.29). Thus the proof is complete.

Remark 4.1 *Solving (4.26) for $\Delta u_{c_i}(t)$ and substituting $u_{c_i}(t)$ from (4.29), one obtains:*

$$
\begin{aligned}
\Delta u_{c_i}(t) &= \frac{1}{\mu_i}(u_{c_i}(t) - u_{ad_i}(t)) \\
&= \frac{1}{\mu_i}\left(\frac{1}{1+\mu_i}\left(u_{ad_i}(t) + \mu_i u_{\max_i}^{\delta_i}\text{sat}\left(\frac{u_{ad_i}(t)}{u_{\max_i}^{\delta_i}}\right)\right) - u_{ad_i}(t)\right) \\
&= \frac{1}{1+\mu_i}\left(u_{\max_i}^{\delta_i}\text{sat}\left(\frac{u_{ad_i}(t)}{u_{\max_i}^{\delta_i}}\right) - u_{ad_i}(t)\right) = \frac{1}{1+\mu_i}\Delta u_{ad_i}^{\delta_i}(t) \qquad (4.32)
\end{aligned}
$$

where $\Delta u_{ad_i}^{\delta_i}(t)$ is introduced for $\Delta u_{ad_i}^{\delta_i}(t) \triangleq u_{\max_i}^{\delta_i}\text{sat}\left(\frac{u_{ad_i}(t)}{u_{\max_i}^{\delta_i}}\right) - u_{ad_i}(t)$. Consequently, if $\Delta u_{ad_i}^{\delta_i}(t)$ is bounded, then the control deficiency $\Delta u_{c_i}(t)$ is inversely proportional to μ_i : $\Delta u_{c_i}(t) = O(1/\mu_i)$.

Lemma 4.4 *The following inequality is true for all $i = 1, ..., m$ and for all $t > 0$:*

$$
u_{c_i}(t)\Delta u_{c_i}(t) \leq 0 \qquad (4.33)
$$

Proof. *If $|u_{c_i}(t)| \leq u_{\max_i}$, then $\Delta u_{c_i}(t) = 0$, and (4.33) holds with the equality sign. If $|u_{c_i}(t)| > u_{\max_i}$, then using (4.14) and the definition for $\Delta u_{c_i}(t)$, we get*

$$
\begin{cases}
u_{c_i}(t) > u_{\max_i}^{\delta_i} \Leftrightarrow \Delta u_{c_i}(t) = u_{\max_i}^{\delta_i} - u_{c_i}(t) < 0 \\
\\
u_{c_i}(t) < -u_{\max_i}^{\delta_i} \Leftrightarrow \Delta u_{c_i}(t) = -u_{\max_i}^{\delta_i} - u_{c_i}(t) > 0
\end{cases} \qquad (4.34)
$$

which implies that $u_{c_i}(t)\Delta u_{c_i}(t) \leq 0$. The proof is complete.

Substituting (4.26) into (4.28) yields the following closed-loop system dynamics:

$$
\dot{\boldsymbol{x}}(t) = (A + B\Lambda K_x^\top(t))\boldsymbol{x}(t) + B\Lambda K_r^\top(t)\boldsymbol{r}(t) + B\Lambda\Delta\boldsymbol{u}_{ad}(t) \qquad (4.35)
$$

where

$$
\Delta\boldsymbol{u}_{ad}(t) \triangleq \mu\Delta\boldsymbol{u}_c(t) + \Delta\boldsymbol{u}(t) = \boldsymbol{u}_{\max}\text{sat}\left(\frac{\boldsymbol{u}_c(t)}{\boldsymbol{u}_{\max}}\right) - \boldsymbol{u}_{ad}(t) \qquad (4.36)
$$

defines the deficiency of the linear in parameters adaptive signal $\boldsymbol{u}_{ad}(t)$.

4.4 Adaptive Reference Model and Matching Conditions

The system dynamics in (4.35) leads to consideration of the following *adaptive* reference model system:

$$\dot{\boldsymbol{x}}_m(t) = A_m \boldsymbol{x}_m(t) + B_m(\boldsymbol{r}(t) + K_u^\top(t)\Delta \boldsymbol{u}_{ad}(t)) \tag{4.37}$$

where $\boldsymbol{x}_m \in \mathbb{R}^m$ is the state of the reference model, A_m is Hurwitz, $K_u(t) \in \mathbb{R}^{m\times m}$ is a matrix of adaptive gains to be determined through stability proof. Comparing (4.37) with system dynamics in (4.35), assumptions are formulated that guarantee existence of the adaptive signal with $\mu-$modification in (4.26).

Assumption 4.1 *(Reference model matching conditions)*

$$\exists K_x^*, \quad K_r^*, \quad K_u^*, \quad B\Lambda(K_x^*)^\top = A_m - A, \quad B\Lambda(K_r^*)^\top = B_m, \quad B_m(K_u^*)^\top = B\Lambda \tag{4.38}$$

Remark 4.2 *The true knowledge of gains K_x^*, K_r^*, K_u^* is not required, only their existence is assumed. The second and third matching conditions in (4.38) imply that $K_u^* K_r^* = I_m$.*

4.5 Stability Analysis

Let $\boldsymbol{e}(t) = \boldsymbol{x}(t) - \boldsymbol{x}_m(t)$ be the tracking error signal. Then, the tracking error dynamics can be written as:

$$\begin{aligned}
\dot{\boldsymbol{e}}(t) &= \dot{\boldsymbol{x}}(t) - \dot{\boldsymbol{x}}_m(t) \\
&= A_m(t)\boldsymbol{e}(t) + B\Lambda\left(\Delta K_x^\top(t)\boldsymbol{x}(t) + \Delta K_r^\top(t)\boldsymbol{r}(t)\right) - B_m \Delta K_u^\top(t)\Delta \boldsymbol{u}_{ad}(t)
\end{aligned} \tag{4.39}$$

where $\Delta K_x(t) = K_x(t) - K_x^*$, $\Delta K_r(t) = K_r(t) - K_r^*$, $\Delta K_u(t) = K_u(t) - K_u^*$ denote parameter errors. Consider the following adaptation laws:

$$\begin{aligned}
\dot{K}_x(t) &= -\Gamma_x x(t)\boldsymbol{e}^\top(t)PB \\
\dot{K}_r(t) &= -\Gamma_r r(t)\boldsymbol{e}^\top(t)PB \\
\dot{K}_u(t) &= \Gamma_u \Delta \boldsymbol{u}_{ad}(t)\boldsymbol{e}^\top(t)PB_m
\end{aligned} \tag{4.40}$$

where $\Gamma_x = \Gamma_x^\top > 0$, $\Gamma_r = \Gamma_r^\top > 0$, $\Gamma_u = \Gamma_u^\top > 0$ are the corresponding matrices of rates of adaptation. Note that for simplicity we have not used $\mathrm{Proj}(\cdot,\cdot)$ while in practice $\mathrm{Proj}(\cdot,\cdot)$ can be used to ensure robustness of parameter errors. In order to assess the closed loop system stability, define the following candidate Lyapunov function:

$$V(\boldsymbol{e}(t), \Delta K_x(t), \Delta K_r(t), \Delta K_u(t)) = \boldsymbol{e}^\top(t) P \boldsymbol{e}(t) + \mathrm{tr}\left(\Delta K_x^\top(t)\Gamma_x^{-1}\Delta K_x(t)\Lambda\right)$$
$$+\mathrm{tr}\left(\Delta K_r^\top(t)\Gamma_r^{-1}\Delta K_r(t)\Lambda\right) + \mathrm{tr}\left(\Delta K_u^\top(t)\Gamma_u^{-1}\Delta K_u(t)\right) \tag{4.41}$$

where $P = P^\top > 0$ solves the algebraic Lyapunov equation

$$A_m^\top P + P A_m = -Q \tag{4.42}$$

for arbitrary $Q = Q^\top > 0$. The time derivative of the Lyapunov function in (4.41) along the system trajectories (4.39), (4.40) is:

$$\begin{aligned}
\dot{V}(t) &= -\boldsymbol{e}^\top(t) Q \boldsymbol{e}(t) + 2\boldsymbol{e}^\top P(B\Lambda(\Delta K_x^\top(t)\boldsymbol{x}(t) + \Delta K_r^\top(t)\boldsymbol{r}(t)) - B_m \Delta K_u^\top(t)\Delta \boldsymbol{u}_{ad}(t)) \\
&+ 2\mathrm{tr}(\Lambda\Delta K_x^\top(t)\Gamma_x^{-1}\Delta\dot{K}_x(t)) + 2\mathrm{tr}(\Lambda\Delta K_r^\top(t)\Gamma_r^{-1}\Delta\dot{K}_r(t)) + 2\mathrm{tr}(\Delta K_u^\top(t)\Gamma_u^{-1}\Delta\dot{K}_u(t)) \\
&= -\boldsymbol{e}^\top(t) Q \boldsymbol{e}(t) + 2\mathrm{tr}\Big(\Lambda\Delta K_x^\top(t)\boldsymbol{x}(t)\boldsymbol{e}^\top(t)PB + \Lambda\Delta K_r^\top(t)\boldsymbol{r}(t)\boldsymbol{e}^\top(t)PB \\
&- \Delta K_u^\top(t)\Delta\boldsymbol{u}_{ad}(t)\boldsymbol{e}^\top(t)PB_m\Big) + 2\mathrm{tr}\Big(\Lambda\Delta K_x^\top(t)\Gamma_x^{-1}\dot{K}_x(t) + \Lambda\Delta K_r^\top(t)\Gamma_r^{-1}\dot{K}_r(t) \\
&+ \Delta K_u^\top(t)\Gamma_u^{-1}\dot{K}_u(t)\Big) \\
&= -\boldsymbol{e}^\top(t) Q \boldsymbol{e}(t) + 2\mathrm{tr}\Big[\Lambda\Delta K_x^\top(t)\Big(\boldsymbol{x}(t)\boldsymbol{e}^\top(t)PB + \Gamma_x^{-1}\dot{K}_x(t)\Big) \\
&+ \Lambda\Delta K_r^\top(t)\Big(\boldsymbol{r}(t)\boldsymbol{e}^\top(t)PB + \Gamma_r^{-1}\dot{K}_r(t)\Big) + \Delta K_u^\top(t)\Big(-\Delta\boldsymbol{u}_{ad}(t)\boldsymbol{e}^\top(t)PB_m + \Gamma_u^{-1}\dot{K}_u(t)\Big)\Big] \\
&= -\boldsymbol{e}^\top(t) Q \boldsymbol{e}(t) + 2\mathrm{tr}\Big[\Lambda\Delta K_x^\top(t)\Big(\boldsymbol{x}(t)\boldsymbol{e}^\top(t)PB - \Gamma_x^{-1}\Gamma_x\boldsymbol{x}(t)\boldsymbol{e}^\top(t)PB\Big) \\
&+ \Lambda\Delta K_r^\top(t)\Big(\boldsymbol{r}(t)\boldsymbol{e}^\top(t)PB - \Gamma_r^{-1}\Gamma_r\boldsymbol{r}(t)\boldsymbol{e}^\top(t)PB\Big) \\
&+ \Delta K_u^\top(t)\Big(-\Delta\boldsymbol{u}_{ad}(t)\boldsymbol{e}^\top(t)PB_m + \Gamma_u^{-1}\Gamma_u\Delta\boldsymbol{u}_{ad}(t)\boldsymbol{e}^\top(t)PB_m\Big)\Big] \\
&= -\boldsymbol{e}^\top(t) Q \boldsymbol{e}(t) \le 0
\end{aligned}$$

Since the derivative of the candidate Lyapunov is negative semidefinite, the signals $\boldsymbol{e}(t)$, $\Delta K_x(t)$, $\Delta K_r(t)$, $\Delta K_u(t)$ are bounded. Hence, there exist $\Delta K_x^{\max}$ and $\Delta K_r^{\max}$ such that $\|\Delta K_x(t)\| < \Delta K_x^{\max}$, $\|\Delta K_r(t)\| < \Delta K_r^{\max} = \alpha \Delta K_x^{\max}$, $\forall t > 0$, where denoting $\alpha = \sqrt{\lambda_{\min}(\Gamma_r)/\lambda_{\min}(\Gamma_x)}$. However, due to the modification of the reference model dynamics in (4.37), one can not conclude stability of the system from above. Consequently one needs in addition prove that one of the signals $\boldsymbol{x}(t)$ or $\boldsymbol{x}_m(t)$ is bounded as well.

Let P_M be the maximum eigenvalue of the matrix P, solving the Lyapunov equation in (4.42), while P_m be the minimum eigenvalue of P. Similarly, let Q_m be the minimum eigenvalue of Q. For the statement of our main result introduce the following notations: $u_{\max} = \max\{u_{\max_1}, u_{\max_2}\}$, $\rho = \frac{P_M}{P_m}$, $\kappa = \left| Q_m - 2\|PB\Lambda\|\|K_x^*\| \right|$, $\omega = u_{\max}\sqrt{m}$, $\varrho = \omega\|U_{\max}^{-1}\|_\infty$, $\eta = Q_m - 2u_{\min}\|U_{\max}^{-1}\|_\infty\|PB\Lambda\|\|K_x^*\|$, $\bar{K}_r = \Delta K_r^{\max} + \|K_r^*\|$, $\bar{K}_x = \Delta K_x^{\max} + \|K_x^*\|$.

Theorem 4.1 *For A and B in (4.12), $u_{\max}$ in (4.14), K_x^*, K_r^* in (4.38) and P and Q in (4.42), let*

$$\mu_1 = \ldots = \mu_m = \mu'$$

$$\mu' < \frac{\eta - \frac{\kappa\rho}{u_{\min}}(\omega + \|U_{\max}^{-1}\|_\infty\|K_r^*\|)}{\frac{\kappa\rho}{u_{\min}}(\omega + \|U_{\max}^{-1}\|_\infty u_{\min}\tilde{u}_{\max} + \tilde{u}_{\max})} \tag{4.43}$$

$$r_{\max} < \frac{\eta - \frac{\kappa\rho}{u_{\min}}\left[\omega(1+\mu') + \mu'\|U_{\max}^{-1}\|_\infty u_{\min}\tilde{u}_{\max} + \mu'\tilde{u}_{\max} + u_{\min}\|U_{\max}^{-1}\|_\infty\|K_r^*\|\right]}{\frac{\kappa\rho}{u_{\min}}\|K_r^*\|} \tag{4.44}$$

If the system initial condition and the initial value of the Lyapunov function in (4.41) satisfy:

$$\boldsymbol{x}^\top(0)P\boldsymbol{x}(0) < P_m\left[\frac{2\|PB\Lambda\|}{\kappa}u_{\min}\right]^2 \tag{4.45}$$

$$\sqrt{V(0)} < \sqrt{\frac{\lambda_{\max}(\Lambda)}{\lambda_{\max}(\Gamma_x)}}$$
$$\frac{\eta - \frac{\kappa\rho}{u_{\min}}\left(\|K_r^*\|r_{\max} + \omega(1+\mu') + u_{\min}\|U_{\max}^{-1}\|_\infty\|K_r^*\| + \mu'\tilde{u}_{\max} + \mu' u_{\min}\tilde{u}_{\max}\|U_{\max}^{-1}\|_\infty\right)}{2u_{\min}\|U_{\max}^{-1}\|_\infty\|PB\Lambda\| + 2\|PB\Lambda\| + \frac{\kappa\rho}{u_{\min}}\alpha r_{\max} + u_{\min}\|U_{\max}^{-1}\|_\infty\alpha} \tag{4.46}$$

where $\lambda_{\max}(\Lambda)$, $\lambda_{\max}(\Gamma_x)$ denote the maximum eigenvalues correspondingly, then

- *the adaptive system in (4.39), (4.40) has bounded solutions $\forall\boldsymbol{r}(t)$, $\|\boldsymbol{r}(t)\| \le r_{\max}$*
- *the tracking error $\boldsymbol{e}(t)$ goes to zero asymptotically,*

$$\boldsymbol{x}^\top(t)P\boldsymbol{x}(t) < P_m\left[\frac{2\|PB\Lambda\|}{\kappa}u_{\max}\sqrt{m}\right]^2, \quad \forall t > 0 \tag{4.47}$$

- $|u_{c_i}(t)| \leq u_{\max_i}$, $i = 1, ..., m$ *that is position saturation of the commanded control signal* $u_{c_i}(t)$ *is overly prevented for all* $t > 0$.

Proof. If $\Delta \boldsymbol{u}(t) = 0$, then the adaptive reference model dynamics in (4.37) reduce to the one in (4.22), and the error dynamics in (4.39) are:

$$\dot{\boldsymbol{e}}(t) = A_m \boldsymbol{e}(t) + B\Lambda \left(\Delta K_x^\top(t)\boldsymbol{x}(t) + \Delta K_r^\top(t)\boldsymbol{r}(t)\right) \tag{4.48}$$

Since (4.22) defines a stable reference model, then $\boldsymbol{x}_m^*(t)$ is bounded. Recall that $\boldsymbol{x}(t) = \boldsymbol{e}(t) + \boldsymbol{x}_m^*(t)$ which ensures that $\boldsymbol{x}(t)$ is bounded. This consequently leads to boundedness of $\dot{\boldsymbol{e}}(t)$, since all terms in (4.48) are bounded. Computing second derivative of $V(t)$ we get

$$\ddot{V}(t) = -2\dot{\boldsymbol{e}}^\top(t) Q \boldsymbol{e}(t)$$

Thus $\ddot{V}(t)$ exists and is bounded since $\boldsymbol{e}(t)$ and $\dot{\boldsymbol{e}}(t)$ are bounded. Therefore, $\dot{V}(t)$ is uniformly continuous. Since, $V(t) > 0$ and $\dot{V}(t) \leq 0$ then $V(t)$ has a finite limit. Using Barbalat's lemma (that states: *if the differentiable function $V(t)$ has a finite limit as $t \to \infty$, and is such that $\ddot{V}(t)$ exists and is bounded, then $\dot{V}(t) \to 0$ as $t \to \infty$.*) together with (4.44), leads to asymptotic convergence of the tracking error $\boldsymbol{e}(t)$ to zero.

If $\Delta \boldsymbol{u}(t) \neq 0$, then in order to prove asymptotic convergence of the tracking error to zero, one needs to show additionally that at least one of the two states $\boldsymbol{x}_m(t)$ or $\boldsymbol{x}(t)$ is bounded. Toward this end, suppose that A is Hurwitz matrix and consider the following candidate Lyapunov function:

$$W(\boldsymbol{x}(t)) = \boldsymbol{x}^\top(t) P_A \boldsymbol{x}(t) \tag{4.49}$$

where $P_A = P_A^\top > 0$ solves the algebraic Lyapunov equation

$$A^\top P_A + P_A A = -Q_A$$

for some positive definite $Q_A > 0$. Since $\Delta \boldsymbol{u}(t) \neq 0$, then $\|\boldsymbol{u}(t)\| \leq u_{\max}\sqrt{m}$, where $u_{\max} = \max\{u_{\max_1}, ..., u_{\max_m}\}$, and the system dynamics in (4.12) become:

$$\dot{\boldsymbol{x}}(t) = A\boldsymbol{x}(t) + B\Lambda \boldsymbol{u}(t) \tag{4.50}$$

Consequently

$$\begin{aligned} \dot{W}(\boldsymbol{x}(t)) &= -\boldsymbol{x}^\top(t) Q_A \boldsymbol{x}(t) + 2\boldsymbol{x}^\top(t) P_A B \Lambda \boldsymbol{u}(t) \\ &\leq -(Q_A)_m \|\boldsymbol{x}(t)\|^2 + 2\|\boldsymbol{x}(t)\| \|P_A B\Lambda\| u_{\max}\sqrt{m} \end{aligned} \tag{4.51}$$

For open-loop stable systems it immediately implies that $\dot{W} < 0$ if $\|\boldsymbol{x}\| > 2\omega\|P_A B\Lambda\|/(Q_A)_m$. Therefore, the system states remain bounded, which results in boundedness of $\dot{\boldsymbol{e}}(t)$. Therefore $\ddot{V}(t)$ is bounded and one can use Barbalat's lemma to conclude that adaptive laws in (4.40) ensure global asymptotic stability of the error dynamics in (4.39).

For unstable systems, i.e. when A is not Hurwitz, add and subtract $B\Lambda(K_x^*)^\top \boldsymbol{x}(t)$ in (4.12) and use the matching assumption in (4.38) to write the system dynamics in the following form:

$$\begin{aligned} \dot{\boldsymbol{x}}(t) &= A\boldsymbol{x}(t) + B\Lambda(K_x^*)^\top \boldsymbol{x}(t) - B\Lambda(K_x^*)^\top \boldsymbol{x}(t) + B\Lambda \boldsymbol{u}(t) \\ &= A_m \boldsymbol{x}(t) - B\Lambda(K_x^*)^\top \boldsymbol{x}(t) + B\Lambda \boldsymbol{u}(t) \end{aligned} \tag{4.52}$$

Consider the following candidate Lyapunov function

$$W(\boldsymbol{x}(t)) = \boldsymbol{x}^\top(t) P \boldsymbol{x}(t), \tag{4.53}$$

where $P = P^\top > 0$ solves the algebraic Lyapunov equation (4.42) for some positive definite $Q > 0$. Then

$$\dot{W}(\boldsymbol{x}(t)) = -\boldsymbol{x}^\top(t) Q x(t) - 2\boldsymbol{x}^\top(t) PB\Lambda(K_x^*)^\top \boldsymbol{x}(t) + 2\boldsymbol{x}^\top(t) PB\Lambda \boldsymbol{u}(t) \tag{4.54}$$

Let

$$u_{\min} = \min\left\{u_{\max_1}, ..., u_{\max_m}\right\}.$$

Notice that $u_{\min} \leq \|\boldsymbol{u}(t)\| \leq \sqrt{m} u_{\max}$ and consider the following two possibilities:

1. $\boldsymbol{x}^\top(t) PB\Lambda \boldsymbol{u}(t) < -\|\boldsymbol{x}(t)\| \|PB\Lambda\| u_{\min}$
2. $\boldsymbol{x}^\top(t) PB\Lambda \boldsymbol{u}(t) \geq -\|\boldsymbol{x}(t)\| \|PB\Lambda\| u_{\min}$

If $\boldsymbol{x}^\top(t) PB\Lambda \boldsymbol{u}(t) < -\|\boldsymbol{x}(t)\| \|PB\Lambda\| u_{\min}$, then from (4.54) we obtain:

$$\begin{aligned} \dot{W}(\boldsymbol{x}(t)) &\leq -Q_m \|\boldsymbol{x}(t)\|^2 + 2\|PB\Lambda\| \|K_x^*\| \|\boldsymbol{x}(t)\|^2 - 2\|\boldsymbol{x}(t)\| \|PB\Lambda\| u_{\min} \\ &\leq \Big| Q_m - 2\|PB\Lambda\| \|K_x^*\| \Big| \|\boldsymbol{x}(t)\|^2 - 2u_{\min} \|PB\Lambda\| \|\boldsymbol{x}(t)\| \end{aligned} \tag{4.55}$$

Therefore, $\dot{W}(\boldsymbol{x}(t)) < 0$ if

$$\boldsymbol{x} \in \mathcal{B}_1 \triangleq \left\{ \boldsymbol{x} \middle| \ \|\boldsymbol{x}\| < 2\|PB\Lambda\| \frac{u_{\min}}{\kappa} \right\} \tag{4.56}$$

Consider the largest set Ω_1 enclosed in $\mathcal{B}_1$, whose boundary forms a level set of $W(\boldsymbol{x}(t))$:

$$\Omega_1 = \left\{ \boldsymbol{x} | \ \ W(\boldsymbol{x}(t)) \leq P_m \left[\frac{2\|PB\Lambda\|u_{\min}}{\kappa} \right]^2 \right\} \tag{4.57}$$

For all initial conditions of $\boldsymbol{x}(t)$ from the set $\mathcal{B}_1$ we have $\dot{W}(\boldsymbol{x}(t)) < 0$, implying that the system states remain bounded.

If $\boldsymbol{x}^\top(t)PB\Lambda\boldsymbol{u}(t) \geq -\|\boldsymbol{x}(t)\|\|PB\Lambda\|u_{\min}$, then using (4.28), we get the following:

$$\begin{aligned} &\boldsymbol{x}^\top(t)PB\Lambda \left[\frac{(I_m+\mu)^{-1}(K_x^\top(t)\boldsymbol{x}(t) + K_r^\top(t)\boldsymbol{r}(t) + \mu\tilde{U}_{\max}\mathrm{sat}(\tilde{U}_{\max}^{-1}\boldsymbol{u}_{ad}(t)))}{\|U_{\max}^{-1}\boldsymbol{u}_c(t)\|_\infty} + \bar{\boldsymbol{u}}(t) \right] \\ + \ \ &\|\boldsymbol{x}(t)\|\|PB\Lambda\|u_{\min} \geq 0 \end{aligned}$$

where $\tilde{U}_{\max}$ is defined in (4.28). Multiplying both sides by 2 we get:

$$\begin{aligned} & 2\boldsymbol{x}^\top(t)PB\Lambda(I_m+\mu)^{-1}(\Delta K_x^\top(t)\boldsymbol{x}(t) + K_r^\top(t)\boldsymbol{r}(t)) \\ + \ & 2\boldsymbol{x}^\top(t)PB\Lambda(I_m+\mu)^{-1}\mu\tilde{U}_{\max}\mathrm{sat}(\tilde{U}_{\max}^{-1}\boldsymbol{u}_{ad}(t)) \\ + \ & 2\boldsymbol{x}^\top(t)PB\Lambda\bar{\boldsymbol{u}}(t) + 2\|U_{\max}^{-1}\boldsymbol{u}_c(t)\|_\infty\|\boldsymbol{x}(t)\|\|PB\Lambda\|u_{\min} \\ \geq \ & -2\boldsymbol{x}^\top(t)PB\Lambda(I_m+\mu)^{-1}(K_x^*)^\top\boldsymbol{x}(t) \end{aligned} \tag{4.58}$$

To continue with the proof one has two choices here. Either setting $\mu_1 = ... = \mu_m = 0$ or let $\mu_1 = ... = \mu_m = \mu'$ and proceed. The first option is a particular case of the second, where $\mu' = 0$. Thus we select the latter leading to

$$(I_m+\mu)^{-1} = \frac{1}{1+\mu'}I_m.$$

Factoring out the constant term $\frac{1}{1+\mu'}$ from the above inequality, one can write (4.58) as follows:

$$\begin{aligned} & 2\boldsymbol{x}^\top(t)PB\Lambda(\Delta K_x^\top(t)\boldsymbol{x}(t) + K_r^\top(t)\boldsymbol{r}(t)) \\ + \ & 2\mu'\boldsymbol{x}^\top(t)PB\Lambda\tilde{U}_{\max}\mathrm{sat}(\tilde{U}_{\max}^{-1}\boldsymbol{u}_{ad}(t)) \\ + \ & 2(1+\mu')\boldsymbol{x}^\top(t)PB\Lambda\bar{\boldsymbol{u}}(t) + 2(1+\mu')\|U_{\max}^{-1}\boldsymbol{u}_c(t)\|_\infty\|\boldsymbol{x}(t)\|\|PB\Lambda\|u_{\min} \\ \geq \ & -2\boldsymbol{x}^\top(t)PB\Lambda(K_x^*)^\top\boldsymbol{x}(t) \end{aligned} \tag{4.59}$$

Writing the derivative of the candidate Lyapunov function as:

$$\dot{W}(\boldsymbol{x}(t)) = -\boldsymbol{x}^\top(t)Q\boldsymbol{x}(t) - 2\boldsymbol{x}^\top(t)PB\Lambda(K_x^*)^\top\boldsymbol{x}(t) + 2\boldsymbol{x}^\top(t)PB\Lambda\boldsymbol{u}(t) \tag{4.60}$$

and substituting for $\bar{\boldsymbol{u}}(t)$ from (4.17) one can upper bound (4.60) as

$$\begin{aligned}\dot{W}(\boldsymbol{x}(t)) &\leq -\boldsymbol{x}^\top(t)Q\boldsymbol{x}(t) + 2\boldsymbol{x}^\top(t)PB\Lambda(\Delta K_x^\top(t)\boldsymbol{x}(t) + K_r^\top(t)\boldsymbol{r}(t))\\ &+ 2\mu'\boldsymbol{x}^\top(t)PB\Lambda\tilde{U}_{\max}\mathrm{sat}(\tilde{U}_{\max}^{-1}\boldsymbol{u}_{ad}(t))\\ &+ 2(1+\mu')\|U_{\max}^{-1}\boldsymbol{u}_c(t)\|_\infty\|\boldsymbol{x}(t)\|\|PB\Lambda\|u_{\min} + 2(1+\mu')\|\boldsymbol{x}(t)\|\|PB\Lambda\|\sqrt{m}u_{\max}\end{aligned} \tag{4.61}$$

Further

$$\tilde{U}_{\max}\mathrm{sat}(\tilde{U}_{\max}^{-1}\boldsymbol{u}_{ad}(t)) = \begin{bmatrix} u_{\max_1}^{\delta_1}\mathrm{sat}\left(\frac{u_{ad_1}(t)}{u_{\max_1}^{\delta_1}}\right)\\ \vdots \\ u_{\max_m}^{\delta_m}\mathrm{sat}\left(\frac{u_{ad_m}(t)}{u_{\max_m}^{\delta_m}}\right)\end{bmatrix},$$

each component of which can be further presented as:

$$u_{\max_i}^{\delta_i}\mathrm{sat}\left(\frac{u_{ad_i}(t)}{u_{\max_i}^{\delta_i}}\right) = \begin{cases} u_{ad_i}(t), & |u_{ad_i}(t)| \leq u_{\max_i}^{\delta_i}\\ u_{\max_i}^{\delta_i}\mathrm{sgn}(u_{ad_i}(t)), & |u_{ad_i}(t)| > u_{\max_i}^{\delta_i}\end{cases} \tag{4.62}$$

with $i = 1, ..., m$. Note that

$$\|\tilde{U}_{\max}\mathrm{sat}(\tilde{U}_{\max}^{-1}\boldsymbol{u}_{ad}(t))\|_2 \leq \|\tilde{U}_{\max}\|_2 \triangleq \tilde{u}_{\max}.$$

Thus, we can further upper bound (4.61) as:

$$\begin{aligned}\dot{W}(\boldsymbol{x}(t)) &\leq -Q_m\|\boldsymbol{x}(t)\|^2 + 2\|\boldsymbol{x}(t)\|\|PB\Lambda\|(\Delta K_x^{\max}\|\boldsymbol{x}(t)\| + \Delta K_r^{\max}r_{\max} + \|K_r^*\|r_{\max})\\ &+ 2(1+\mu')\|\boldsymbol{x}(t)\|\|PB\Lambda\|\sqrt{m}u_{\max} + 2(1+\mu')\|U_{\max}^{-1}\boldsymbol{u}_c(t)\|_\infty\|\boldsymbol{x}(t)\|\|PB\Lambda\|u_{\min}\\ &+ 2\mu'\|\boldsymbol{x}(t)\|\|PB\Lambda\|\|\tilde{U}_{\max}\mathrm{sat}(\tilde{U}_{\max}^{-1}\boldsymbol{u}_{ad}(t))\|_2\end{aligned}$$

Further,

$$
\begin{aligned}
\dot{W}(\boldsymbol{x}(t)) &\leq -Q_m\|\boldsymbol{x}(t)\|^2 + 2\|\boldsymbol{x}(t)\|\|PB\Lambda\|(\Delta K_x^{\max}\|\boldsymbol{x}(t)\| + \Delta K_r^{\max} r_{\max} + \|K_r^*\| r_{\max}) \\
&+ 2(1+\mu')\|\boldsymbol{x}(t)\|\|PB\Lambda\|\sqrt{m}u_{\max} + 2(1+\mu')\|U_{\max}^{-1}\|_\infty\|\boldsymbol{u}_c(t)\|_\infty\|\boldsymbol{x}(t)\|\|PB\Lambda\|u_{\min} \\
&+ 2\mu'\|\boldsymbol{x}(t)\|\|PB\Lambda\|\underbrace{\|\tilde{U}_{\max}\|_2}_{\tilde{u}_{\max}}
\end{aligned}
$$

Since $\|\boldsymbol{u}_c(t)\|_\infty \leq \|\boldsymbol{u}_c(t)\|_2$ we can rewrite the above as

$$
\begin{aligned}
\dot{W}(\boldsymbol{x}(t)) &\leq -Q_m\|\boldsymbol{x}(t)\|^2 + 2\|\boldsymbol{x}(t)\|\|PB\Lambda\|(\Delta K_x^{\max}\|\boldsymbol{x}(t)\| + \Delta K_r^{\max} r_{\max} + \|K_r^*\| r_{\max}) \\
&+ 2(1+\mu')\|\boldsymbol{x}(t)\|\|PB\Lambda\|\sqrt{m}u_{\max} + 2(1+\mu')\|U_{\max}^{-1}\|_\infty\|\boldsymbol{u}_c(t)\|_2\|\boldsymbol{x}(t)\|\|PB\Lambda\|u_{\min} \\
&+ 2\mu'\|\boldsymbol{x}(t)\|\|PB\Lambda\|\tilde{u}_{\max}
\end{aligned} \tag{4.63}
$$

Substituting for $u_{c_i}(t)$ from (4.28) and using the definition of $\tilde{u}_{\max}$ we get

$$
\begin{aligned}
\dot{W}(\boldsymbol{x}(t)) &\leq -Q_m\|\boldsymbol{x}(t)\|^2 + 2\|\boldsymbol{x}(t)\|\|PB\Lambda\|(\Delta K_x^{\max}\|\boldsymbol{x}(t)\| + \Delta K_r^{\max} r_{\max} + \|K_r^*\| r_{\max}) \\
&+ 2(1+\mu')\|\boldsymbol{x}(t)\|\|PB\Lambda\|\sqrt{m}u_{\max} + 2\|U_{\max}^{-1}\|_\infty(\|K_x(t)\|\|\boldsymbol{x}(t)\| + \|K_r(t)\|\|\boldsymbol{r}(t)\|) \\
&\quad \|\boldsymbol{x}(t)\|\|PB\Lambda\|u_{\min} + 2\mu'\|U_{\max}^{-1}\|_\infty\|\tilde{U}_{\max}\mathrm{sat}(\tilde{U}_{\max}^{-1}\boldsymbol{u}_{ad}(t))\|_2\|\boldsymbol{x}(t)\|\|PB\Lambda\|u_{\min} \\
&+ 2\mu'\|\boldsymbol{x}(t)\|\|PB\Lambda\|\tilde{u}_{\max}
\end{aligned} \tag{4.64}
$$

and upper bounding further yields:

$$
\begin{aligned}
\dot{W}(\boldsymbol{x}(t)) &\leq -Q_m\|\boldsymbol{x}(t)\|^2 + 2\|\boldsymbol{x}(t)\|\|PB\Lambda\|(\Delta K_x^{\max}\|\boldsymbol{x}(t)\| + \Delta K_r^{\max} r_{\max} + \|K_r^*\| r_{\max}) \\
&+ 2(1+\mu')\|\boldsymbol{x}(t)\|\|PB\Lambda\|\sqrt{m}u_{\max} + 2\|U_{\max}^{-1}\|_\infty((\Delta K_x^{\max} + \|K_x^*\|)\|\boldsymbol{x}(t)\| \\
&+ (\Delta K_r^{\max} + \|K_r^*\|)r_{\max})\|\boldsymbol{x}(t)\|\|PB\Lambda\|u_{\min} \\
&+ 2\mu'\|\boldsymbol{x}(t)\|\|PB\Lambda\|\tilde{u}_{\max} + 2\mu'\|U_{\max}^{-1}\|_\infty\tilde{u}_{\max}\|\boldsymbol{x}(t)\|\|PB\Lambda\|u_{\min}
\end{aligned} \tag{4.65}
$$

where the subindex 2 has been dropped from the norm. Further, grouping the terms, one gets:

$$\begin{aligned}
\dot{W}(\boldsymbol{x}) &\leq -\Big(Q_m - 2\|PB\Lambda\|\Delta K_x^{\max} - 2u_{\min}\|U_{\max}^{-1}\|_\infty\|PB\Lambda\|(\Delta K_x^{\max} + \|K_x^*\|)\Big)\|\boldsymbol{x}\|^2 \\
&+ 2\|\boldsymbol{x}\|\|PB\Lambda\|\Big((\Delta K_r^{\max} + \|K_r^*\|)r_{\max} + \sqrt{m}(1+\mu')u_{\max} \\
&+ u_{\min}\|U_{\max}^{-1}\|_\infty(\Delta K_r^{\max} + \|K_r^*\|)r_{\max} + \mu'\tilde{u}_{\max} + \mu'\|U_{\max}^{-1}\|_\infty\tilde{u}_{\max}u_{\min}\Big) \qquad (4.66)
\end{aligned}$$

Notice that since $V(\boldsymbol{e}(t), \Delta K_x(t), \Delta K_r(t), \Delta K_u(t))$ is radially unbounded, and its derivative is negative, then the maximal values of all errors, including $\Delta K_x^{\max}$,$\Delta K_r^{\max}$, do not exceed the level set value of the Lyapunov function $V = V_0 = V(0)$. Therefore using the assumed inequality (4.46) yields:

$$\Delta K_x^{\max} < \frac{\eta - \frac{\kappa\rho}{u_{\min}}\Big(\|K_r^*\|r_{\max} + \omega(1+\mu') + u_{\min}\|U_{\max}^{-1}\|_\infty\|K_r^*\| + \mu'\tilde{u}_{\max} + \mu' u_{\min}\tilde{u}_{\max}\|U_{\max}^{-1}\|_\infty\Big)}{2u_{\min}\|U_{\max}^{-1}\|_\infty\|PB\Lambda\| + 2\|PB\Lambda\| + \frac{\kappa\rho}{u_{\min}}\alpha r_{\max} + u_{\min}\|U_{\max}^{-1}\|_\infty\alpha} \qquad (4.67)$$

This in turn guarantees that $Q_m - 2\|PB\Lambda\|\Delta K_x^{\max} - 2u_{\min}\|U_{\max}^{-1}\|_\infty\|PB\Lambda\|(\Delta K_x^{\max} + \|K_x^*\|) > 0$. Consequently, it follows from (4.66) that $\dot{W}(\boldsymbol{x}(t)) < 0$ if

$$\begin{aligned}
&\|\boldsymbol{x}\| \geq \\
&2\|PB\Lambda\|\Big[\frac{(\Delta K_r^{\max} + \|K_r^*\|)r_{\max} + \sqrt{m}(1+\mu')u_{\max} + u_{\min}\|U_{\max}^{-1}\|_\infty(\Delta K_r^{\max} + \|K_r^*\|)r_{\max}}{Q_m - 2\|PB\Lambda\|\Delta K_x^{\max} - 2u_{\min}\|U_{\max}^{-1}\|_\infty\|PB\Lambda\|(\Delta K_x^{\max} + \|K_x^*\|)} \\
&+\frac{\mu'\tilde{u}_{\max} + \mu'\|U_{\max}^{-1}\|_\infty\tilde{u}_{\max}u_{\min}}{Q_m - 2\|PB\Lambda\|\Delta K_x^{\max} - 2u_{\min}\|U_{\max}^{-1}\|_\infty\|PB\Lambda\|(\Delta K_x^{\max} + \|K_x^*\|)}\Big] = \Theta
\end{aligned}$$

Define the ball

$$\mathcal{B}_2 = \{\boldsymbol{x}| \ \ \|\boldsymbol{x}\| \leq \Theta\}$$

and the smallest set Ω_2 that encloses $\mathcal{B}_2$, the boundary of which is a level set of the Lyapunov function $W(\boldsymbol{x}(t))$:

$$\Omega_2 = \left\{\boldsymbol{x}| \ \ W(\boldsymbol{x}(t)) \leq P_M\Theta^2\right\}$$

By rearranging the terms in (4.67)

$$\sqrt{P_M}\frac{\Theta}{2\|PB\Lambda\|} \leq \sqrt{P_m}\frac{u_{\min}}{\kappa}$$

and consequently $\Omega_2 \subset \Omega_1$, implying that there exists an annulus region $\Omega_1 \setminus \Omega_2 \neq \emptyset$. Thus our analysis of the closed-loop system dynamics reveals that when $\Delta\boldsymbol{u}(t) \neq 0$, there always exists a *non-empty* annulus region such that $\dot{W}(\boldsymbol{x}(t)) < 0$ holds $\forall \boldsymbol{x}$ from that region. In other words, asymptotic convergence of the tracking error to zero and boundedness of all signals are guaranteed as long as the system initial conditions satisfy (4.45) and initial parameter errors comply with (4.46).

Remark 4.3 *Inequality in (4.44) ensures that the resulting numerator in (4.46) is positive.*
Remark 4.4 *Theorem 3.5 implies that if the initial conditions of the state and parameter errors lie within certain bounds, then the adaptive system will have bounded solutions. The local nature of the result for* unstable *system is due to the static actuator model constraints (4.14) imposed on the control input. For open-loop stable systems the results are global.*
Remark 4.5 The condition in (4.46) can be viewed as an upper bound for α, which limits the choice of the adaptation gains Γ_x and Γ_r.

It remains only to show that the control signal will never incur saturation. Thus from (4.32) it follows that $\Delta u_{c_i}(t)$ can be upper bounded as

$$|\Delta u_{c_i}(t)| \leq \frac{u^{\delta_i}_{\max_i} + (\Delta K^{\max}_x + \|K^*_x\|)\|\boldsymbol{x}(t)\| + (\Delta K^{\max}_r + \|K^*_r\|)r_{\max}}{1+\mu'}$$

and

$$|\Delta u_{c_i}(t)| \leq \frac{\overbrace{u^{\delta_i}_{\max_i} + 2(\Delta K^{\max}_x + \|K^*_x\|)\|PB\Lambda\|\frac{u_{\min}}{\kappa} + (\Delta K^{\max}_r + \|K^*_r\|)r_{\max}}^{C}}{1+\mu'}$$

By definition $\Delta u_{c_i}(t) = u^{\delta_i}_{\max_i}\mathrm{sat}\left(\frac{u_{c_i}(t)}{u^{\delta_i}_{\max_i}}\right) - u_{c_i}(t), \quad i = 1, ..., m$. Hence, $|\Delta u_{c_i}(t)| \geq |u_{c_i}(t)| - \left|u^{\delta_i}_{\max_i}\mathrm{sat}\left(\frac{u_{c_i}(t)}{u^{\delta_i}_{\max_i}}\right)\right|$, and consequently $|u_{c_i}(t)| \leq u^{\delta_i}_{\max_i} + \frac{C}{1+\mu'}$. Let $\tilde{\delta} = \min\{\delta_i\}$, and since $\mu' > 0$, one can satisfy $\frac{C}{1+\mu'} < \tilde{\delta}$. Recalling that $u^{\delta_i}_{\max_i} = u_{\max_i} - \delta$, one arrives at

$$\mu' > \frac{u_{\min}(\kappa + 2\|PB\Lambda\|(\Delta K^{\max}_x + \|K^*_x\|) + (\Delta K^{\max}_r + \|K^*_r\|)\kappa r_{\max}}{\kappa\tilde{\delta}} - 2 \tag{4.68}$$

Remark 4.6 Setting $\delta_i = \delta$ results in a simpler design, while may reduce the conservative lower bound on μ'.

Chapter 5

Applications and Simulations

5.1 F-16 and missile Simulations

Consider F-16 short-period dynamics data at sea level, airspeed of 502 ft/s, and angle of attack of 2.11 degrees:

$$A_{\text{nom}} = \begin{bmatrix} -1.0189 & 0.9051 \\ 0.8223 & -1.0774 \end{bmatrix},$$
$$\boldsymbol{b} = \begin{bmatrix} -0.0022 \\ -0.1756 \end{bmatrix}, \quad \boldsymbol{c} = [0\ 1]^\top. \tag{5.1}$$

Open-loop system eigenvalues are: $\lambda_1 = -0.1850$ and $\lambda_2 = -1.9113$. The *Ricatti* equation is solved with the following weight matrices:

$$Q = \begin{bmatrix} 8 & 0 \\ 0 & 0.5 \end{bmatrix}, \quad r = 0.01, \tag{5.2}$$

resulting in the following linear optimal gains $\boldsymbol{k}_{lqr} = [-16.3706\ \ -9.7194]^\top$, leading to the closed loop eigenvalues: $\lambda_{1,2} = -1.92 \pm 1.03i$.

Figure 5.1 shows tracking of the reference model pitch rate $q_{\text{ref}}(t)$ in response to $r^{\text{cmd}} = 17\sin(t)$ by the LQR controller in the absence of failures and saturation. Next, we introduce the following failures:

- 50 % elevator effectiveness failure $\Rightarrow M_{\delta_f} = 0.5 M_\delta, Z_{\delta_f} = 0.5 Z_\delta$

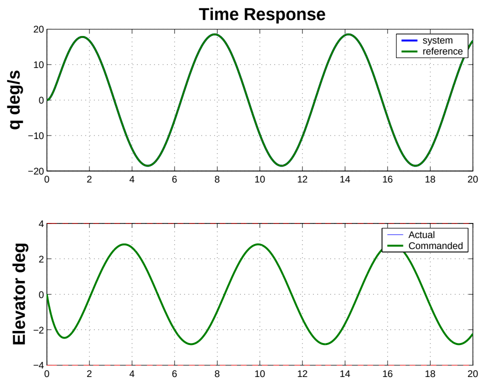

Figure 5.1: LQR performance with no uncertainty: response to sinusoidal input

- 50 % increase in static instability $\Rightarrow M_{\alpha_f} = 1.5M_\alpha$
- Nonlinear matched uncertainty in the pitching moment

$$f(\alpha) = \alpha^3 - (\exp(-10(10\alpha + 0.5)^2) - \exp(-10(10\alpha - 0.5)^2) + 0.5\sin(2\alpha)$$

Figure 5.2 shows performance degradation of the baseline LQR controller.

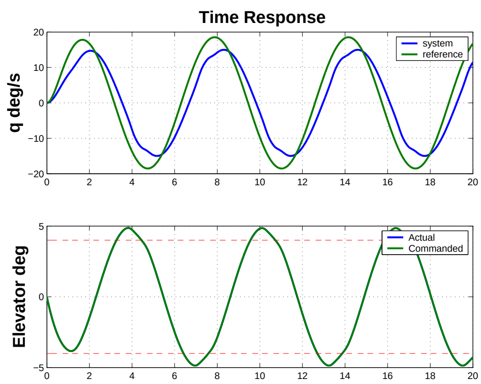

Figure 5.2: LQR performance in the presence of uncertainties: response to sinusoidal input in the absence of actuator limits

In order to cope with the system uncertainties, we design MRAC controller and simulate it without enforcing the saturation limits (see Fig. 5.3). Rates of adaptation and Q_0 matrix in the Lyapunov equation were chosen as:

$$\Gamma_x = \begin{bmatrix} 5 & 0 \\ 0 & 10 \end{bmatrix}, \quad Q_0 = \begin{bmatrix} 1 & 0 \\ 0 & 250 \end{bmatrix}$$

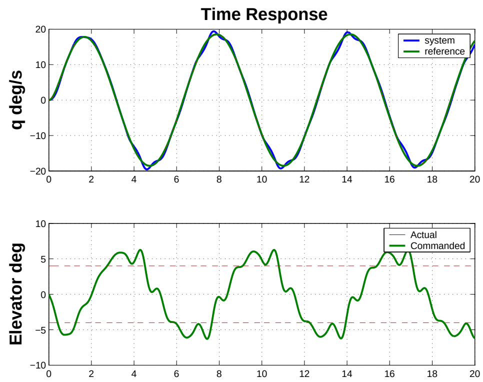

Figure 5.3: Performance of adaptive controller ignoring the saturation limits

Next, the same adaptive controller is simulated in the presence of control limits. The result is shown in Figure 5.4. As seen from the Figure, the control signal saturates but does not

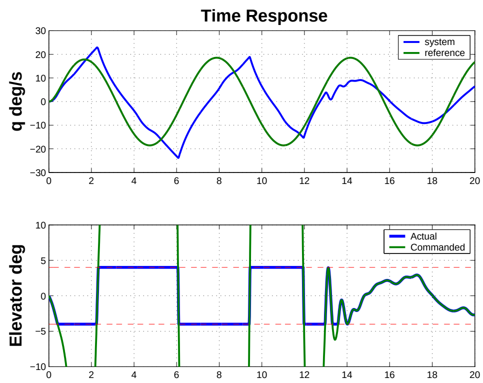

Figure 5.4: Adaptive control performance in the presence of saturation

destabilize the system. This is consistent with the theory, as the open-loop nominal aircraft model in (5.1) is stable. To avoid saturation, we try two different values of $\mu = 0$, and $\mu = 15$. The results are shown in Figure 5.5 and Figure 5.6. Figure 5.5 presents the tracking performance of the adaptive control architecture from [12], when $\mu = 0$. It is clear in this case that tracking is recovered using *modified* reference command. When $\mu = 15$ is selected positive μ-mod prevents saturation at all times with slightly modifying reference command. Note that one can either iterate to obtain the desired value of μ or use the lower bound of

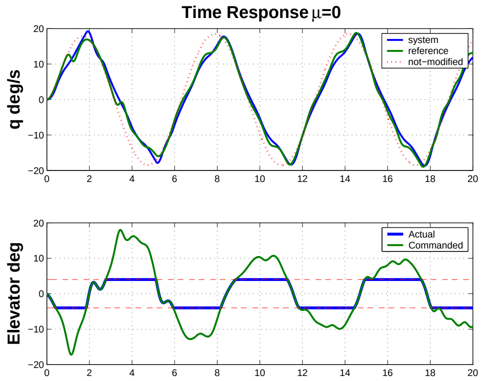

Figure 5.5: Adaptive control with $\mu = 0$-modification

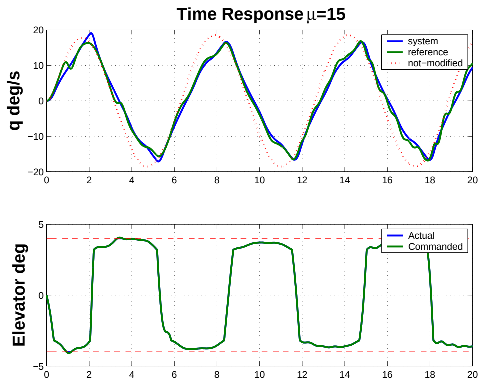

Figure 5.6: Adaptive control with $\mu = 15$-modification

that is given in [16]. In this case, rates of adaptation are set to:

$$\Gamma_x = \begin{bmatrix} 5 & 0 \\ 0 & 10 \end{bmatrix}$$

$\gamma_r = 5$, $\gamma_u = 0.01$, and

$$\Gamma_\theta = \begin{bmatrix} 2 & 0 \\ 0 & 2 \end{bmatrix}.$$

Next, we present simulation results for an open-loop system that represents a generic missile short-period dynamics. The missile data are:

$$A_{\text{nom}} = \begin{bmatrix} -1.3046 & 1 \\ 32.7109 & -20 \end{bmatrix},$$

$$\boldsymbol{b} = \begin{bmatrix} -0.0037 \\ -1.8297 \end{bmatrix}, \quad \boldsymbol{c} = [1 \ 0]^\top .$$

Open-loop system eigenavlues are:

$$\lambda_1 = 0.3063, \lambda_2 = -21.6109 .$$

In this example, we design an angle of attack (AoA) autopilot. The following weighting matrices

$$Q = \begin{bmatrix} 40 & 0 \\ 0 & 0 \end{bmatrix}, \quad r = 0.04$$

are used for solving the Riccatti equation, which lead to the following closed-loop optimal eigenvalues:

$$\lambda_1 = -2.8275, \lambda_2 = -21.4276$$

The Lyapunov equation for adaptive control is solved with

$$Q_0 = \begin{bmatrix} 250 & 0 \\ 0 & 1 \end{bmatrix}.$$

We consider the following failures

- 30 % elevator effectiveness failure $\Rightarrow M_{\delta_f} = 0.7M_\delta, Z_{\delta_f} = 0.7Z_\delta$
- 30 % increase in static instability $M_{\alpha_f} = 1.3M_\alpha$
- Nonlinear matched uncertainty in the pitching moment

$$f(\alpha) = \alpha^3 - (\exp(-10(10\alpha + 0.5)^2) - \exp(-10(10\alpha - 0.5)^2) + 0.5\sin(2\alpha)$$

Figure 5.7 shows tracking performance of the LQR controller in the absence of uncertainties. The degradation of the tracking performance in the presence of uncertainties is shown in Figure 5.8.

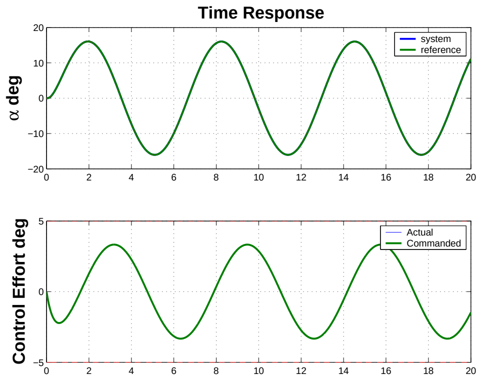

Figure 5.7: LQR performance in the absence of uncertainties and actuation limits

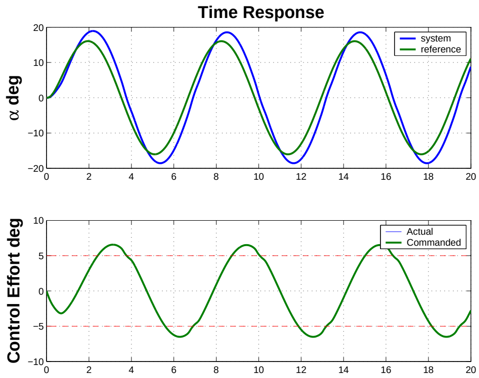

Figure 5.8: LQR performance in the presence of uncertainties

Next adaptive control is used to compensate for uncertainties, and the results are shown in Figure 5.9. The data indicate that tracking is recovered with commanded control effort. This leads to actuator position saturation. Performance degradation of adaptive controller in the presence of saturation is plotted in Figure 5.10.

In order to decrease commanded control values, μ-modification based adaptive control is implemented, and time responses are shown in Figure 5.11 ($\mu = 0$) and Figure 5.12 ($\mu = 4$).

Rates of adaptation were set to:

$$\Gamma_x = \begin{bmatrix} 190 & 0 \\ 0 & 10 \end{bmatrix}, \ \Gamma_\theta = \begin{bmatrix} 1.2 & 0 \\ 0 & 1.2 \end{bmatrix}, \ \gamma_r = 15,$$

$$\gamma_u = 0.01$$

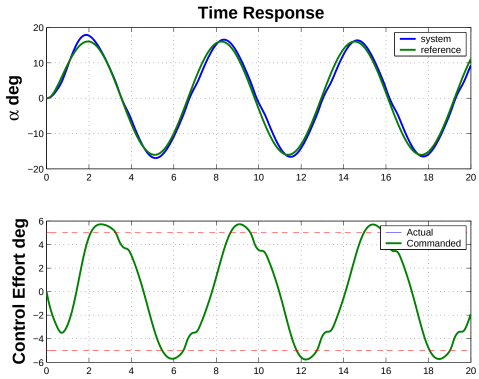

Figure 5.9: Recovery of the performance with adaptive controller in the presence of uncertainties without actuation limits

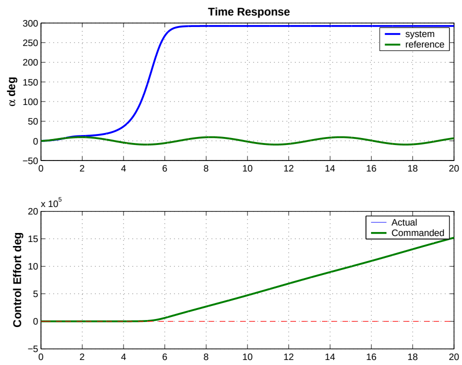

Figure 5.10: Adaptive control performance in the presence of saturation

Figure 5.12 shows that control effort is decreased due to reference model modification, and saturation is prevented overall when the value of μ is chosen appropriately large.

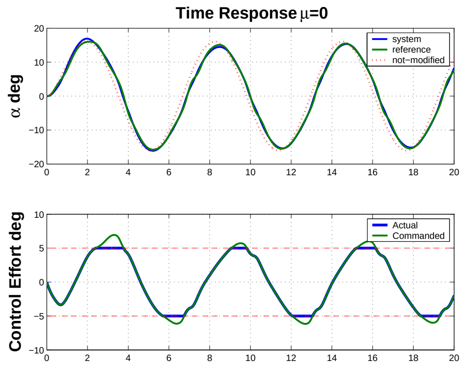

Figure 5.11: Missile response with μ=0

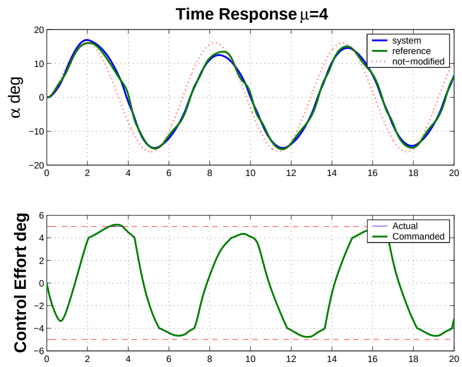

Figure 5.12: Missile response with μ=4

5.2 Multi-Input System

Consider the short period dynamics of an airplane with an additional control input

$$\begin{bmatrix} \dot{\alpha}(t) \\ \dot{q}(t) \end{bmatrix} = \begin{bmatrix} Z_\alpha & \cos(\theta_0) \\ M_\alpha & M_q \end{bmatrix} \begin{bmatrix} \alpha(t) \\ q(t) \end{bmatrix} + \begin{bmatrix} Z_\delta & Z_N \\ M_\delta & M_N \end{bmatrix} \begin{bmatrix} \delta(t) \\ \delta_{\text{Nozzle}}(t) \end{bmatrix} \tag{5.3}$$

$$y = \begin{bmatrix} 1 & 0 \\ 0 & 1 \end{bmatrix} \begin{bmatrix} \alpha \\ q \end{bmatrix} = [\alpha \quad q]^\top \tag{5.4}$$

where δ_{Nozzle} can be used to control pitch motion along with elevator input δ_e. Thrust vectoring is another example of two control inputs. Leading edge or trailing edge flaps are another

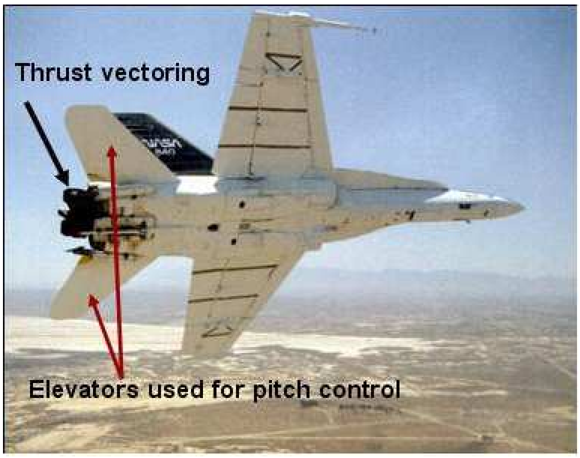

Figure 5.13: Elevators and Nozzles used for pitch control.

examples where more that one control input is used for pitch control. For the subject of multi-input simulations we have chosen an F-18 Harv fighter flying at altitude of 15000 ft, Mach 0.7, and trim AoA of 2.52. The system's matrices are:

$$A = \begin{bmatrix} -1.0817 & 0.99 \\ 1.5943 & -0.5936 \end{bmatrix}, \quad B = \begin{bmatrix} -0.0031 & -0.0003 \\ -0.2241 & -0.0278 \end{bmatrix}$$

where eigenvalues of A are $\lambda_1 = -2.1163, \quad \lambda_2 = 0.4410$. Thus this model is unstable and therefore is an interesting candidate to examine our theory.

5.3 Constructing the Multi-Input Reference Model

The reference model here is chosen such that A_m is Hurwitz, and B_m is:

$$B_m = \begin{bmatrix} 1 & 0 \\ 0 & 1 \end{bmatrix}, \quad \boldsymbol{r}^{\text{cmd}} = \begin{bmatrix} r_\delta \\ r_{\text{Nozzle}} \end{bmatrix} \tag{5.5}$$

We choose the reference model to have

$$A_m = \begin{bmatrix} -2.4 & -1.8 \\ 1.8 & -2.4 \end{bmatrix},$$

leading to the following eigenvalues

$$\lambda_{1,2} = -2.4 \pm 1.8i.$$

The reference model in (4.37) takes the form:

$$\underbrace{\begin{bmatrix} \dot{\alpha} \\ \dot{q} \end{bmatrix}}_{\dot{\boldsymbol{x}}_m(t)} = \underbrace{\begin{bmatrix} -2.4 & -1.8 \\ 1.8 & -2.4 \end{bmatrix}}_{A_m} \underbrace{\begin{bmatrix} \alpha \\ q \end{bmatrix}}_{\boldsymbol{x}_m(t)} + \underbrace{\begin{bmatrix} 1 & 0 \\ 0 & 1 \end{bmatrix}}_{B_m} \left(\underbrace{\begin{bmatrix} r_\delta \\ r_{Nozzle} \end{bmatrix}}_{\boldsymbol{r}^{\text{cmd}}(t)} + K_u^\top(t)\Delta u_{ad}(t) \right)$$

5.4 Simulations for Tracking in Multi-Input Systems

At first, we assume no uncertainties in the system and let the adaptive controller only stabilize the system and track the states of the reference model while tuning the gains for closer tracking of pitch rate. It should be noted that both states can be tracked. However, since the control influence on AoA is very weak one would need large feedforward gains to achieve perfect AoA tracking (large gains are undesirable while close tracking of AoA is not necessary in airplanes). The tracking is shown in Figure 5.14 when $\boldsymbol{r}^{\text{cmd}}(t)$ is:

$$\boldsymbol{r}^{\text{cmd}}(t) = \begin{bmatrix} 9(\sin(2t) + \sin(0.5t) + \sin(t) + \sin(0.25t)) \\ 12\sin(2t) \end{bmatrix}$$

It can be seen that the adaptive controller is stabilizing and tracking the reference model without exceeding the saturation limits of the elevator and nozzle. These saturation limits are given as follows:

- $-88 \ \text{deg} \leq \delta_e \leq 88 \ \text{deg}$
- $-15 \ \text{deg} < \delta_{\text{Nozzle}} < 15 \ \text{deg}$

Then we consider the following two failure cases.

5.4.1 First Class of Failures

First simulate the system with the adaptive controller in the presence of the following uncertainties

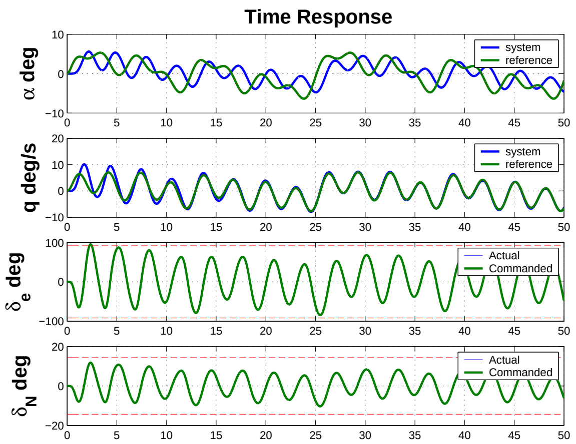

Figure 5.14: Adaptive controller tracking in the absence of uncertainties.

- 50 % elevator effectiveness
- 50 % nozzle effectiveness

while not enforcing the saturation limits. The result is shown in Figure 5.15. As it can be

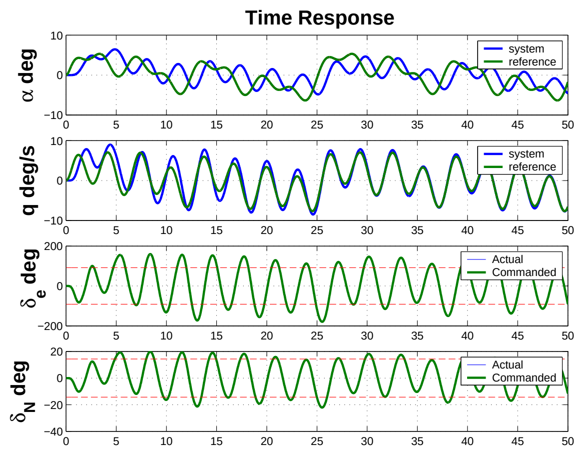

Figure 5.15: Adaptive controller in the presence of uncertainties and absence of saturation limits.

seen from Figure 5.15, that the adaptive controller has been able to recover the tracking while its control effort has increased in both channels such that they exceed the allowable amplitude limits. The adaptive gains used for the purpose of simulations are

$$\Gamma_x = \begin{bmatrix} 10 & 0 \\ 0 & 30 \end{bmatrix}, \quad \Gamma_r = \begin{bmatrix} 10 & 0 \\ 0 & 20 \end{bmatrix}$$

and

$$Q = \begin{bmatrix} 200 & 0 \\ 0 & 300 \end{bmatrix}.$$

Next we like to see how adaptive control copes when saturation limits are enforced. Figure 5.16 shows how the system tends to instability when saturation occurs. We implement

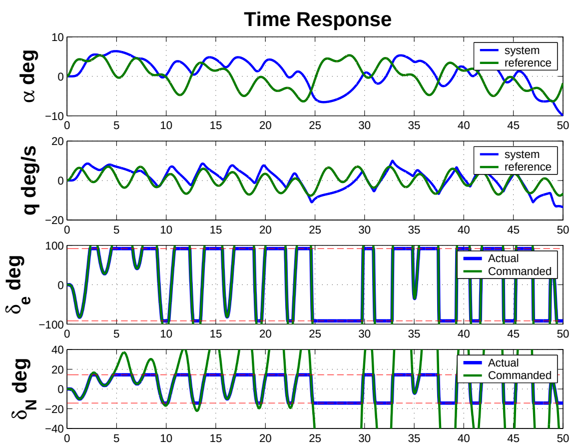

Figure 5.16: Adaptive controller in the presence of saturation limits

positive μ-mod modification for two different values of $\mu' = 0$ and $\mu' = 3.5$. Figure 5.17 shows the first case.

It is clear from Figure 5.17 that stability is recovered in the system while reference system is modified such that the system now can track the modified reference model. This means that we ask the guidance system to reduce the demand on the reference input such that the controller is able to track the reference command without leading to instability. In the later case of μ' we can achieve tracking not only by recovering stability but by completely avoiding the saturation. Figure 5.18 shows that reference model is modified so that the control effort never incurs saturation. The value of μ' can be adjusted, however it can never exceed a certain upper bound. This means that for certain value of μ' system becomes unstable again. Thus one must be cautious when increasing the value of μ'. Also note that due to stability analysis we have used the same value of μ' and $\delta = 20\% u_{\max}$. For the purpose of

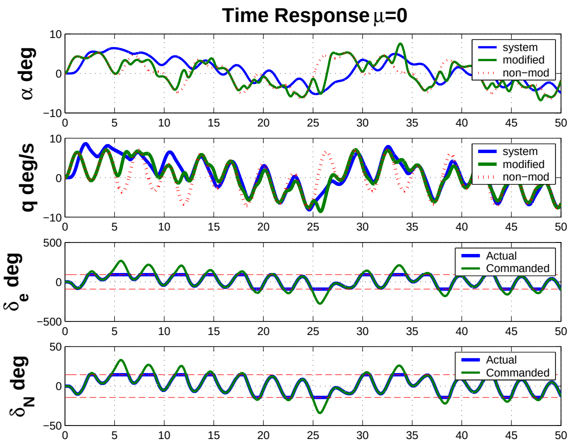

Figure 5.17: Positive-μ implemented when $\mu' = 0$

these simulation we selected Γ_u to be

$$\Gamma_u = \begin{bmatrix} 0.01 & 0 \\ 0 & 0.01 \end{bmatrix}.$$

5.4.2 Second Class of Failures

Second we consider additional failures in the system. We make the pitch stiffness more positive. This means that the center of gravity of the airplane is not calculated by the flight computer accurately or there are some computing failures. Also, we keep the elevator effectiveness low to simulate battle damages or environmental effects on the elevator. Thus the summary of failures are as follow:

- 50 % elevator effectiveness $\delta_f = 0.5\delta$
- 75 % nozzle effectiveness $\delta_{\mathrm{Nozzle_f}} = 0.75\delta_{\mathrm{Nozzle}}$
- 30 % increase in static instability $M_{\alpha_f} = 1.3M_\alpha$

It can be seen from Figure 5.19 that the plant becomes less stable. While the level of uncertainty is not known to the control system, positive μ-mod modification can maintain the tracking without saturating the system.

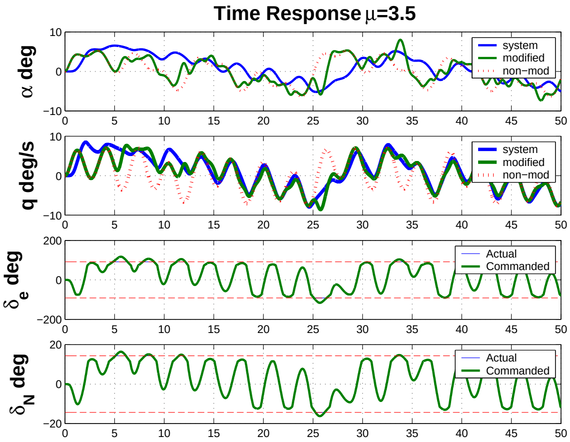

Figure 5.18: Positive-μ implemented when $\mu' = 3.5$

5.4.3 Multiple States Tracking

Next we show application of positive μ-mod to track closely two states using two control inputs. The linearized lateral/directional model of an airplane in stability axis is given as

$$\begin{bmatrix} \dot{\beta} \\ \dot{p} \\ \dot{r} \\ \dot{\phi} \end{bmatrix} = \underbrace{\begin{bmatrix} \frac{Y_\beta}{V} & \frac{Y_p}{V} & -(1-\frac{Y_r}{V}) & \frac{g\cos(\theta_0)}{V} \\ L_\beta & L_p & L_r & 0 \\ N_\beta & N_p & N_r & 0 \\ 0 & 1 & 0 & 0 \end{bmatrix}}_{A} \begin{bmatrix} \beta \\ p \\ r \\ \phi \end{bmatrix} + \underbrace{\begin{bmatrix} 0 & \frac{Y_{\delta_r}}{V} \\ L_{\delta_a} & L_{\delta_r} \\ N_{\delta_a} & N_{\delta_r} \\ 0 & 0 \end{bmatrix}}_{B} \begin{bmatrix} \delta_a \\ \delta_r \end{bmatrix}$$

$$y = \begin{bmatrix} 1 & 0 & 0 & 0 \\ 0 & 0 & 0 & 1 \end{bmatrix} \begin{bmatrix} \beta \\ p \\ r \\ \phi \end{bmatrix} = [\beta \quad \phi]^\top.$$

For our simulation we use the lateral/directional model of A-4D flying at Mach 0.4 at sea level. The model matrices are given as follow:

$$A = \begin{bmatrix} -0.0247 & 0 & -1.0000 & 0.0721 \\ -2.2963 & -0.1682 & 0.0808 & 0 \\ 1.3483 & -0.0036 & -0.0589 & 0 \\ 0 & 1 & 0 & 0 \end{bmatrix}, \quad B = \begin{bmatrix} 0 & 0.0043 \\ 1.7437 & -2.1847 \\ 0.4258 & 0.0884 \\ 0 & 0 \end{bmatrix}$$

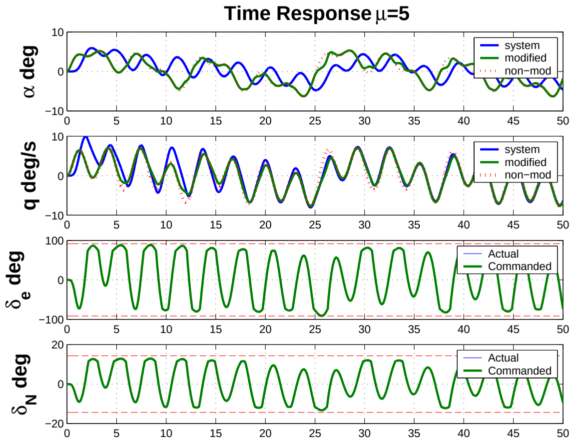

Figure 5.19: Positive-μ implemented when $\mu' = 5$. In the presence of new uncertainties and addition of control failures μ-mod prevents saturation while maintains tracking

The eigenvalues of this model are:

$$\begin{aligned}\lambda_{1,2} &= 0.0200 \pm 1.1722i \\ \lambda_3 &= -0.2869 \\ \lambda_4 &= -0.0048\end{aligned}$$

Note that the Dutch-Roll mode is unstable and the roll mode has very long time constant. Next we select our reference model such that Dutch-Roll is stable. The reference A_m and B_m are

$$A_m = \begin{bmatrix} -0.0357 & 0.0013 & -1.0270 & 0.0743 \\ -0.5702 & -2.5783 & 6.6766 & -0.6469 \\ 0.1831 & -0.4096 & -2.3557 & 0.1607 \\ 0 & 1 & 0 & 0 \end{bmatrix}, \quad B_m = \begin{bmatrix} 0 & 0 \\ 1 & 0 \\ 1 & 1 \\ 0 & 0 \end{bmatrix}$$

The eigenvalues of the reference model are:

$$\begin{aligned}\lambda_{1,2} &= -2.40 \pm 1.80i \\ \lambda_3 &= -0.1217 \\ \lambda_4 &= -0.0480\end{aligned}$$

For the purpose of tracking we introduce a step input of 10 degrees in both channels for a period of 3 seconds. Then we introduce a distributed control failure with the following Λ:

$$\Lambda = \begin{bmatrix} 0.6 & 0 & 0 & 0 \\ 0 & 0.6 & 0 & 0 \\ 0 & 0 & 0.7 & 0 \\ 0 & 0 & 0 & 0.6 \end{bmatrix}$$

The control failure mainly means 65% of ailerons and rudder are effective. We select the following actuator amplitude limits:

- $-29 \leq \delta_a \leq 29 \ \ \text{deg}$
- $-34 \leq \delta_r \leq 34 \ \ \text{deg}$

and design a linear in parameter adaptive control with following adaptive gains and Lyapunov weighting matrix:

$$\Gamma_x = \begin{bmatrix} 15 & 0 & 0 & 0 \\ 0 & 10 & 0 & 0 \\ 0 & 0 & 20 & 0 \\ 0 & 0 & 0 & 20 \end{bmatrix}, \quad \Gamma_r = \begin{bmatrix} 9 & 0 \\ 0 & 5 \end{bmatrix}, \quad Q = \begin{bmatrix} 200 & 0 & 0 & 0 \\ 0 & 100 & 0 & 0 \\ 0 & 0 & 200 & 0 \\ 0 & 0 & 0 & 1 \end{bmatrix}.$$

The adaptive control design compensates for control failures while it demands higher control efforts than actuators can offer. Figure 5.20 shows the adaptive controller in the absence of saturation limits. It can be seen that the adaptive controller demands higher control efforts than actuators limits.

Next saturation limits are set to observe the effect of actuator saturation on adaptive system. The resultant simulation is shown in Figure 5.21.

It can be seen from Figure 5.21 that the system becomes unstable in the presence of saturation limits. Next we use positive μ-mod to recover tracking of reference states and prevent saturation. Figure 5.22 shows the results when $\mu' = 40$.

It can be seen from Figure 5.22 that stability and tracking are recovered for sideslip and bank angle while saturation is prevented in both channels. The value of Γ_u for positive

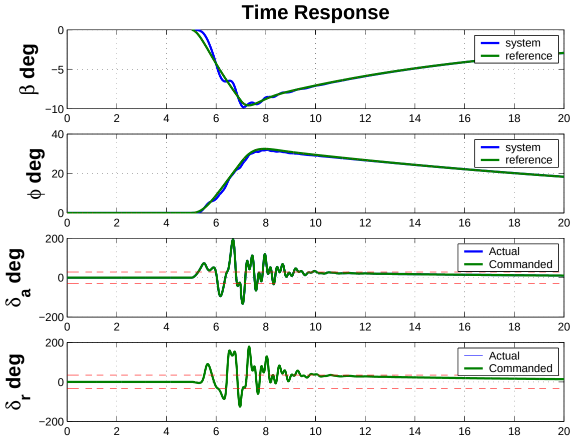

Figure 5.20: Adaptive controller in the presence of control failures and absence of saturation limits.

μ-modification is:

$$\Gamma_u = \begin{bmatrix} 0.01 & 0 \\ 0 & 0.01 \end{bmatrix}.$$

5.5 Summary

In this chapter we presented applications of positive μ-mod method to aircraft and missiles. First the formulated single input μ-mod technique was applied to a stable F-16 and an unstable hypothetical missile. The results showed satisfactory tracking in the presence of amplitude actuator saturation. The tracking was achieved by modifying the reference command by the adaptive parameter $K_u(t)$. Next, we showed application of the positive μ-mod technique for multi-input systems. Two examples of such a system were an unstable F-18 and an unstable A4-D. In F-18 thrust vectoring and elevators to tightly track pitch rate and loosely track angle of attack and in A4-D aileron and rudder were used to closely track sideslip and bank angle. For F-18 the results showed that for a case when both elevator and nozzle are only 50 percent effective, positive μ-mod recovers the stability and tracking of the system while the adaptive controller copes with failures of the control systems and uncertainties of derivatives. In A4-D simulations showed that tracking and stability are recovered and actuator saturation is prevented in both channels when positive μ-mod is implemented. The tracking was achieved while control saturation was prevented when μ' was selected using (4.68). The simulations also showed that increasing the value of μ' can

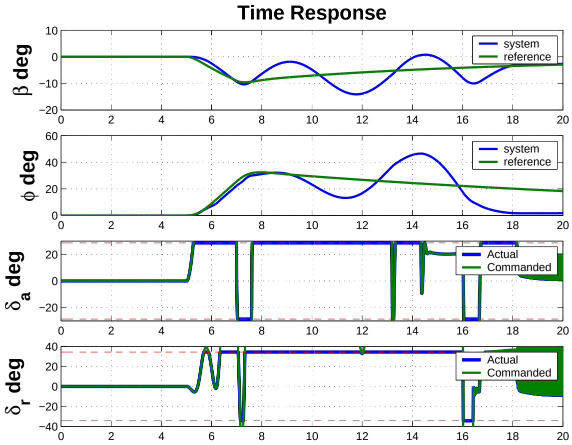

Figure 5.21: Adaptive controller in the presence of control failures and input saturation.

cause system instability. Thus the upper bound on μ' needs to be determined before any algorithm is applied.

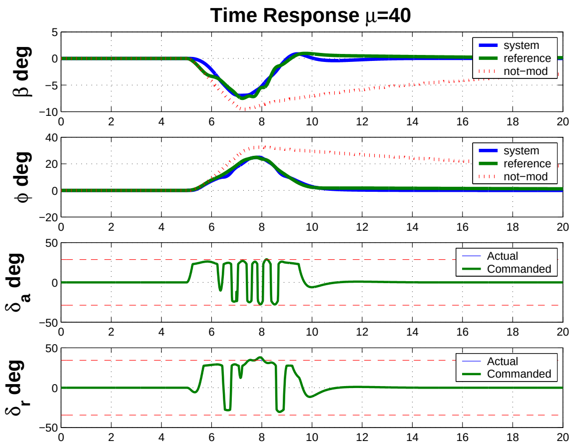

Figure 5.22: Positive-μ implemented when $\mu' = 40$. In the presence of control failures μ-mod prevents saturation while maintains tracking and recovers stability.

Chapter 6

Summary, Conclusion and Recommendations

6.1 Summary and Conclusion

The changes in structures, and systems of an airplane or missile require adaptive control laws to guarantee stable performance of tracking. Even though adaptive controllers provide reasonable tracking and performance, they may demand higher control effort that can be achieved by actuators. Incurring saturation causes loss of tracking in stable systems, or loss of stability in unstable systems. Thus a powerful technique is needed with constructive stability proofs to help recover the tracking in the presence of amplitude saturation. Examples of single input or multi-input systems are present in many aerospace applications. Therefore, it is important to have constructive stability proofs for any adaptive controller that is formulated for single input or multi-input systems. On the other hand, stability proofs for multi-input systems require different approach from a single input case.

The difficulty arises when one needs to find a lower bound for states of the system in a multiple input systems. Therefore, the values of μ needed to be either zero or equal such that it can be factored out as a scalar. The resultant algorithm was an extension of [16] that was introduced for a single input system. The results showed that if the conditions (4.43), (4.45), and (4.46) are satisfied there always exists a non empty region such that if system states are initialized within that region stability can be achieved while using maximum possible control authority. In many cases positive μ-mod can prevent actuator saturation as well.

The constructive Lyapunov based stability analysis showed that the system can maintain stability for a stable or unstable system. Then the technique of [16] was applied to stabilize and track the pitch rate and angle of attack of an F-16 and a hypothetical missile. The results of the multi-input system were also applied to unstable A4-D and F-18 to track the commanded inputs while stability was recovered in the presence of amplitude saturation. It is important to note that when uncertainties or control surface failures are introduced in the system, adaptive controllers are able to recover the stability and tracking at the price of increased control efforts. This in turn causes instability for unstable A4-D, F-18, missile and loss of tracking for stable F-16 when saturation limits are enforced. Multi-input and single input positive μ-modification recovered the stability and tracking by modifying the reference command and consequently states of the reference model. Also, it was noted that the weighting matrix in solving the Lyapunov equation needed to be considerably large to ensure stability of the system. The value Γ_u needed to be selected as small as possible so that smallest modifications are made in the reference model to prevent saturation or recover stability of the system. The value of μ' could not also exceed a certain level since it could violate the condition in (4.43).

6.2 Recommendations

After considering the benefits of positive μ-mod which gives the control system the ability of using its maximum control authority, in some cases the initial parameter error or domain of attraction becomes so small that positive μ-mod may not be effective. This condition in domain of attraction and upper bound on parameter errors needs to be verified before any simulation or application of positive μ-mod is considered. This means that there is a certain level of uncertainties in A or values of Λ that positive μ-mod can handle. The process of applying positive μ-mod usually starts by first finding the saturation limits where adaptive controller becomes unstable. Then, positive μ-mod is applied and the value of μ is slowly increased until the desired performance is achieved. In the mean time, if the system shows undesirable behavior, it is recommended that first the compoeenents of Γ_u be adjusted without changing any other adaptation gains. In case of application and simulation issues, it is recommended that when positive μ-mod is applied the smallest possible step size of integration be used to prevent from any numerical instability in the system. Also, due to condition in (4.44) one needs to be cautious to make sure the guidance or autopilot never issues commands higher than $r_{\max}$. At the end and for most, it should be noted that an unstable system that provides sufficient domain of attraction for positive μ-mod requires some damping in the system. Thus systems without any damping have such a small domain of attraction that positive μ-mod may not be applicable to them.

6.2.1 Future Work

Often dynamics of actuators are so complicated that their dynamics need be included in the stability proofs. Also, the position of actuators are not measurable. Thus a model of actuator needs to be constructed to estimate the position of actuator at any instance. This will also require careful stability proofs to ensure stability of the system when the estimated actuator position is used in positive μ-modification.

Bibliography

[1] D.Y. Abramovitch, R.L. Kosut, and G.F. Franklin. Adaptive control with saturating inputs. *In Proceedings of* 25^{th} *IEEE Conference on Decision and Control*, pp. 848–852, 1986.

[2] D.Y. Abramovitch and G.F. Franklin. On the Stability Adaptive Poles-PLacement Controllers with a Saturating Actuator . *IEEE Transactions on Automatic Control* , 35(3): 303–304, 1990.

[3] M.R. Akella, J.L. Junkins, R.D. Robinett. Structured Model Reference Adaptive Control with Actuator Saturation Limits. *AIAA Guidance, Navigation, and Control Conference and Exhibit*, No. A98-37381. 1998.

[4] D. Bernstein and A. A. Michel. Chronological bibliography on saturating actuators. *International Journal of Robust and Nonlinear Control*, 5:375–380, 1995.

[5] J.D. Boskovic, S. Liand and R.K. Mehran. Robust Adaptive Variable Structure Control of Spacecraft Under Control Input Saturation. *Journal Guidance, Control, and Dynamics*, 24(1), January-February 2001.

[6] J.B. Burl. Linear Optimal Control. *Addison-Wesley Longman*, California, 1999.

[7] F.Z. Chaoui, F. Giri, L. Dugard, J.M. Dion and M. M'saad. Adaptive Tracking with Saturating INput and Controller INtegral Action . *IEEE Transactions on Automatic Control* , 43(11): 1638–1643, 1998.

[8] W. Durham. Aircrfat Dynamics and Control Class Notes. , Virginia Tech, Blacksburg, VA 2004.

[9] E. Farrell, M. Polycarpou, and M. Sharma. On-line approximation based control of uncertain nonlinear systems with magnitude, rate and bandwidth constraints on the

states and actuators. *In Proceedings of American Control Conference*, Boston, MA, pp. 2257-2562, 2004.

[10] G. Feng, C. Zhang and M. Palaniswami. Adaptive Pole Placement Control Subject to Input Amplitude Constraints. *Proceedings of the 30th Conference on Decesion and Control* , Brighton, England. December 1991.

[11] E. N. Johnson and A. J. Calise. Limited authority adaptive flight control for reusable lunch vehicles. *Journal of Guidance, Control and Dynamics*, 26:906–913, 2003.

[12] S.P. Karason and A.M. Annaswamy. Adaptive control in the presence of input constraints. *IEEE Transactions on Automatic Control*, 39:2325–2330, 1994.

[13] S.K. Kannan and E. Johnson. Adaptive Control with a Nested Stauration Reference Model. *AIAA Guidance, Navigation, and Control Conference and Exhibit* ,No. AIAA 2003-5324, Austin, TX, August 2003.

[14] M. Kanamori and M. Tomizuka. Model Reference Adaptive Control of Linear Systems with Input Saturation. *Proceedings of the 2004 IEEE INternational Conference on Control Applications* ,Taipei, Taiwan, September 2-4, 2004.

[15] M. Krstic,I. Kanellakopoulos, P. Kokotovic. Nonlinear and Adaptive Control Design. *Wiley Internscience*, New York, 1995.

[16] E. Lavretsky and N. Hovakimyan. Positive μ-modification for stable adaptation in the presence of input constraints. *In Proceedings of American Control Conference*, pp. 2545 - 2550, 2004.

[17] E. Lavretsky, N. Hovakimyan. Positive μ-modification for stable adaptation in a class of nonlinear systems with actuator constraints. *Submitted to International Journal of Adaptive Control and Signal Processing*, 2003.

[18] A. Leonessa, W. Haddad, and T. Hayakawa. Adaptive tracking for nonlinear systems with input constraints. *In Proceedings of American Control Conference*, Washington DC, pp. 1292-1297, 2001.

[19] R. Monopoli. Adaptive control for systems with hard saturation. *In Proceedings of* 14^{th} *IEEE Conference on Decision and Control*, Houston, TX, pp.841–843, 1975.

[20] R.C. Nelson. Flight Stability and Automatic Control. *McGraw-Hill*, New York, 1998.

[21] F. Ohkawa and Y. Yonezawa. A discrete model reference adaptive control system for a plant with input amplitude constraints. *International Journal of Control*, 36:747–753, 1982.

[22] A.N. Payne. Adaptive one-step-ahead control subject to input-amplitude constraint. *International Journal of Control*, 43:1257–1269, 1986.

[23] J.B. Pomet and L. Praly. Adaptive Nonlinear Regulation: Estimation from the Lyapunov Equation. *IEEE Transactions on Automatic Control*, 37(6):729–740, 1992.

[24] R. Sanner and J.J. Slotine. Gaussian networks for direct adaptive control. *IEEE Transactions on Neural Networks*, 3(6):837–864, 1992.

[25] M. Schwager. Towards Verifiable Adptive Control for Safety Critical Applications. *M.S Thesis*, Massachusetts Institute of Technology, 2005.

[26] B.L. Stevens, F.L. Lewis Aircrfat Control and Simulation. *Wiley*, New York, 2003.

[27] M. Tandale and J. Valasek. Structured Adaptive Model Inversion Control to Simultaneosly Handle Actuator Failure and Actuator Saturation. *AIAA Guidance, Navigation, and Control Conference and Exhibit* ,No. AIAA 2003-5325, Austin, TX, August 2003.

[28] C. Zhang and R.J. Evans. Amplitude constrained adaptive control. *International Journal of Control*, 46:53–64, 1987.